



**HAL**  
open science

# Implementation of Operators via Filter Banks; Hardy Wavelets and Autocorrelation Shell

Gregory Beylkin, Bruno Torresani

► **To cite this version:**

Gregory Beylkin, Bruno Torresani. Implementation of Operators via Filter Banks; Hardy Wavelets and Autocorrelation Shell. Applied and Computational Harmonic Analysis, 1995, 3, pp.164-185. 10.1006/acha.1996.0014 . hal-01223132

**HAL Id: hal-01223132**

**<https://hal.science/hal-01223132>**

Submitted on 2 Nov 2015

**HAL** is a multi-disciplinary open access archive for the deposit and dissemination of scientific research documents, whether they are published or not. The documents may come from teaching and research institutions in France or abroad, or from public or private research centers.

L'archive ouverte pluridisciplinaire **HAL**, est destinée au dépôt et à la diffusion de documents scientifiques de niveau recherche, publiés ou non, émanant des établissements d'enseignement et de recherche français ou étrangers, des laboratoires publics ou privés.

# IMPLEMENTATION OF OPERATORS VIA FILTER BANKS; Hardy Wavelets and Autocorrelation Shell

G. Beylkin\* and B. Torr sani†

November 13, 1995

## Abstract

We consider implementation of operators via filter banks in the framework of the Multiresolution Analysis. Our method is particularly efficient for convolution operators. Although our method of applying operators to functions may be used with any wavelet basis with a sufficient number of vanishing moments, we distinguish two particular settings, namely, orthogonal bases, and the autocorrelation shell.

We apply our method to evaluate the Hilbert transform of signals and derive a fast algorithm capable of achieving any given accuracy. We consider the case where the wavelet is the autocorrelation function of another wavelet associated with an orthonormal basis and where our method provides a fast algorithm for the computation of the modulus and the phase of signals. Moreover, the resulting wavelet may be viewed as being (approximately, but with any given accuracy) in the Hardy space  $H^2(\mathbb{R})$ .

## I INTRODUCTION

In this paper we introduce a method for design of digital filters and consider their implementation and application via filter banks. The design of digital filters is always a trade-off between accuracy and efficiency. For a number of operators this trade-off obtained via traditional filter design techniques is not adequate, especially if high precision is required. As examples, consider the Hilbert transform or operators of fractional differentiation where an accurate traditional implementation over a wide band necessarily implies a long filter.

Signal processing is not the only field where fast and accurate implementation of such operators is of interest. In numerical analysis Fast Multipole Method (FMM) [18, 9, 4] has been developed to address this problem. Although this method proved to be efficient in numerical analysis, it did not so far find its way into the signal processing. A possible explanation for this may be the traditional reliance on filtering operations in the signal processing community. In fact, multiresolution techniques evolved in signal processing as subband coding techniques [8, 20]. The original motivation for subband coding was essentially optimal representation and compression of signals. The introduction of the orthonormal bases of wavelets [21, 16] and the concept of multiresolution analysis [13, 15] have led to the development of a broader concept of harmonic analysis of signals where subband coding became a natural way of representing and analyzing signals. These notions also migrated to numerical analysis, where they

---

\*Program in Applied Mathematics, University of Colorado, Boulder, Colorado 80304, USA

†CPT, CNRS-Luminy, Case 907, 13288 Marseille Cedex 09, France

were applied to the problem of efficient representation and application of operators [3]. In particular, it was shown in [3] how to use wavelet bases to “almost diagonalize” certain classes of operators, for example, pseudodifferential and Calderón-Zygmund operators. For signal processing applications the approach of [3] is also of interest. Although designed for numerical purposes, algorithms of [3] explicitly use quadrature mirror filters (QMFs) with the “exact reproduction property” and may be viewed as a link between signal processing techniques and traditional numerical computing.

The method developed in this paper is different from that of [3] and may be also easily implemented both in software and hardware. It avoids the construction of non-standard forms which, although quite efficient, are not as simple as the “filter banks approach” described in this paper. Briefly, we decompose a signal into different scales (subbands) and implement operators as subband filters. Let us, for example, consider a convolution operator  $T$ . The wavelet  $\psi$  may be written as

$$\hat{\psi}(\xi) = m_1(\xi/2) \hat{\phi}(\xi/2),$$

where  $\hat{\psi}$  and  $\hat{\phi}$  are the Fourier transform of the wavelet and of the scaling function. The  $2\pi$ -periodic square-integrable function  $m_1$  represents one of the Quadrature Mirror Filters (QMFs). Our approach is based on an observation that if the wavelet  $\psi(x)$  is sufficiently well localized in the Fourier domain, one may write

$$(\widehat{T\psi})(\xi) \approx m_T(\xi/4) \hat{\phi}(\xi/4), \tag{1.1}$$

where  $m_T$  is a  $2\pi$ -periodic function which is computed given the symbol of the operator  $T$ . The accuracy of the approximation in (1.1) is controlled by the number of vanishing moments of the wavelet  $\psi$  (it might be necessary to consider (1.1) on each scale separately if the symbol of  $T$  is not homogeneous). As a result, the operator  $T$  is implemented using filters  $m_T$  (may be different on different scales), where  $m_T$  plays a role similar to that of the filter  $m_1$  of the QMF pair. The major difference, which is already visible in equation (1.1), is that the  $m_T$  filter performs a scaling by a factor 4 instead of 2. This has some practical implications, which are discussed throughout the paper. The factor 4 may be replaced by a factor  $2^n$ ,  $n \geq 2$ , as a way to improve accuracy. In this way, the procedure for design of these subband filters allows us to attain any desired accuracy.

The approach of this paper (as that of [3]) may be traced back to Calderón-Zygmund and Littlewood-Paley approach to harmonic analysis of functions and operators which we apply here to design filters given the symbol of an operator. Our method may be used with any wavelets (associated with quadrature mirror filters) which possess sufficient number of vanishing moments. In cases where the associated scaling function also has vanishing moments (which implies that the corresponding coefficients are well approximated by samples on fine scales), our algorithm leads to a fast method for computing the Hilbert transform (and, thus, modulus and phase) of signals. This is the case for the autocorrelation wavelets derived in [19] which we consider here in some detail. Although our approach is quite general, we concentrate on several specific examples, such as the Hilbert transform, operators of differentiation and, more generally, convolution operators. In particular, we consider the Hilbert transform both as an example and an important special case, because of its particular status (it is one of the simplest and most popular examples of Calderón-Zygmund operators) and its relevance in signal processing. In our approach the Hilbert transform (as well as a number of other operators) is completely expressed in terms of filter banks, which makes it easy to handle for a wide variety of scientific communities. In addition to the Hilbert transform, we construct derivative and integration operators including those of fractional order.

Our approach also allows us to consider the following related problem. In signal processing it is often useful to deal with wavelets that belong to the complex Hardy space  $H^2(\mathbb{R})$ , i.e., wavelets such that their Fourier transform is zero for negative frequencies. For instance, such wavelets are considered to be more efficient for the identification of “chirps” (i.e. amplitude and frequency modulated components) in signals. In particular, it is easy to identify the “carrier” frequency and remove it by shifting in the frequency domain if necessary. However, there does not exist any orthonormal multiresolution analysis of  $H^2(\mathbb{R})$  where the associated wavelet has such a property [1]. Nevertheless, as we show in this paper, it is possible to keep the algorithmic structure of multiresolution analysis and use wavelets that approximate the Hilbert transform of a given real-valued function with any given (but finite) accuracy. The sum of the original wavelet and  $i$  times its approximate Hilbert transform yields a new wavelet that is approximately in  $H^2(\mathbb{R})$ . As a direct consequence, we obtain a fast algorithm for the computation of the Hilbert transform, and a pyramidal algorithm for discrete wavelet transform with complex analytic (or progressive) wavelet [10]. This may be thought of as a starting point to carry on an analysis similar to that developed in [6, ?, 12].

The first part of the paper is devoted to the representation of operators in terms of filter banks. To illustrate our approach, we derive in Section II the function  $m_T$  in (1.1) for the Hilbert transform. We then present in Section III a general approach of filter banks implementation of convolution operators (in these two sections, we consider compactly supported orthogonal wavelets and obtain  $O(N)$  algorithms). We then turn to the particular case of the autocorrelation of Daubechies’ compactly supported wavelets in Section IV. We again consider first the Hilbert transform and then, in Section V, develop approximations of other operators (e.g., operators of fractional differentiation and integration) by our technique.

In the second part of the paper we address the signal processing problems using autocorrelation wavelets. In Section VI we consider computing the Hilbert transform as well as modulus and phase of signals and, in Section VII, address the problem of decomposition of band-pass signals into amplitude and frequency modulated components. The main tools are the same as in the first part of the paper, namely filter banks implementation of Hilbert transform. However, the algorithm we describe is  $O(N \log N)$  since we choose to use a translation-invariant version of wavelet transform. Finally, Section VIII is devoted to conclusions.

## II THE HILBERT TRANSFORM

As a way of introduction, let us consider our approach for implementing the Hilbert transform,

$$(\mathcal{H}f)(x) = \frac{1}{\pi} \text{p.v.} \int_{-\infty}^{\infty} \frac{f(s)}{x-s} ds. \quad (2.1)$$

The general case and some other operators will be considered in the following sections.

Let us start with the usual MRA (see Appendix). It is well known that the Hilbert transform of the wavelet  $\psi(x)$  is still a wavelet. Since we will be interested in computing coefficients  $\langle \mathcal{H}f, \psi_k^j \rangle$ , let us consider the function  $\mathcal{H}^* \psi$  given in the Fourier domain by

$$\begin{aligned} (\widehat{\mathcal{H}^* \psi})(\xi) &= i \operatorname{sgn}(\xi) \hat{\psi}(\xi) \\ &= i \operatorname{sgn}(\xi) m_1\left(\frac{\xi}{2}\right) \hat{\phi}\left(\frac{\xi}{2}\right), \end{aligned} \quad (2.2)$$

where  $\mathcal{H}^*$  denotes the adjoint of  $\mathcal{H}$ . Let us consider the  $4\pi$ -periodic function

$$m_2(\xi) = i \sum_k \operatorname{sgn}(\xi + 4\pi k) m_1(\xi + 4\pi k) \chi_{[-2\pi, 2\pi]}(\xi + 4\pi k). \quad (2.3)$$

Our main observation is as follows: although  $i \operatorname{sgn}(\xi) m_1(\xi)$  is not a periodic function, the product  $i \operatorname{sgn}(\xi) m_1(\xi) \hat{\phi}(\xi)$  may be well approximated by  $m_2(\xi) \hat{\phi}(\xi)$ , due to the fast decay of  $\hat{\phi}(\xi)$ .

**Proposition II.1** 1. *The Fourier coefficients  $b_\ell$  of the function*

$$m_2(\xi) = \frac{1}{\sqrt{2}} \sum_\ell b_\ell e^{i\ell\xi/2}$$

are given by

$$b_\ell = \begin{cases} -\frac{1}{\pi} \sum_k \frac{g_k}{k - \frac{\ell}{2}} & \text{for odd } \ell \\ 0 & \text{for even } \ell \end{cases} \quad (2.4)$$

2. *The Fourier coefficients  $b_\ell$  have the following asymptotics*

$$b_{2\ell-1} \sim O((2\ell-1)^{-M-1}) \quad (2.5)$$

Notice that asymptotics (2.5) coincides with the asymptotics expected from the general approach of [3].

*Proof:*

1. Consider the Fourier coefficients of  $m_2(\xi)$

$$b_\ell = \frac{i\sqrt{2}}{4\pi} \int_{-2\pi}^{2\pi} m_1(\xi) \operatorname{sgn}(\xi) e^{-i\ell\xi/2} d\xi \quad (2.6)$$

$$= \frac{i}{4\pi} \int_0^{2\pi} \left[ m_1(\xi) e^{-i\ell\xi/2} - m_1(-\xi) e^{i\ell\xi/2} \right] d\xi \quad (2.7)$$

$$= -\frac{1}{2\pi} \sum_k g_k \int_0^{2\pi} \sin\left(k - \frac{\ell}{2}\right) \xi d\xi \quad (2.8)$$

which yields (2.4).

2. The decay of the coefficients  $b_{2\ell-1}$  is governed by the regularity of  $m_2(\xi)$  at the origin, *i.e.* by the number of vanishing moments of the wavelet. The asymptotics (2.5) is obtained using Taylor series expansion of (2.4) and taking into account the vanishing moments of the sequence  $\{g_\ell\}$ :

$$b_{2\ell-1} = -\frac{1}{\pi} \sum_k \frac{g_k}{k - \frac{2\ell-1}{2}} \quad (2.9)$$

$$= \frac{2}{\pi} \sum_k \frac{g_k}{2\ell-1} \sum_{p=0}^{\infty} \left( \frac{2k}{2\ell-1} \right)^p \quad (2.10)$$

$$= \frac{2}{\pi} \sum_k \frac{g_k}{2\ell-1} \sum_{p=M}^{\infty} \left( \frac{2k}{2\ell-1} \right)^p \quad (2.11)$$

$$\sim O((2\ell-1)^{-M-1}) \quad (2.12)$$

which proves (2.5).

In other words, the Hilbert transform is essentially a local operator on functions which have sufficient number of vanishing moments.

**Remarks:**

1. We notice that the sequence  $\{b_{2\ell-1}\}$  may be viewed as the Hilbert transform of the sequence  $\{g_k\}$ . We note that for sequences the singular behaviour of the Hilbert transform at the origin is avoided by the  $\frac{1}{2}$  term in the denominator, and the slow decay at infinity is replaced by (2.5).
2. A statement similar to Proposition II.1 may be proved for wavelets with rational  $m_0$  and  $m_1$ . Let

$$m_1(\xi) = \frac{P(e^{i\xi})}{Q(e^{i\xi})} \quad (2.13)$$

be a rational  $2\pi$ -periodic function, where both  $P$  and  $Q$  are polynomials. Set  $p(\xi) = P(e^{i\xi})$ ,  $q(\xi) = Q(e^{i\xi})$  and consider

$$p_2(\xi) = i \sum_k \operatorname{sgn}(\xi + 4\pi k) p(\xi + 4\pi k) \chi_{[-2\pi, 2\pi]}(\xi + 4\pi k), \quad (2.14)$$

and the  $4\pi$ -periodic function

$$m_2(\xi) = \frac{p_2(\xi)}{q(\xi)} \quad (2.15)$$

Since  $p(\xi)$  carries all the vanishing moments of  $m_1(\xi)$ , the quality of the approximation of  $i \operatorname{sgn}(\xi) m_1(\xi) \hat{\phi}(\xi)$  by  $m_2(\xi) \hat{\phi}(\xi)$  is controlled by that of the approximation of  $i \operatorname{sgn}(\xi) p(\xi) \hat{\phi}(\xi)$  by  $p_2(\xi) \hat{\phi}(\xi)$ . Such approximation was discussed in Proposition II.1.

Using Proposition II.1, we obtain from (2.2) the following approximation

$$(\widehat{\mathcal{H}^* \psi})(\xi) \approx m_{\mathcal{H}^*}(\xi/4) \hat{\phi}(\xi/4), \quad (2.16)$$

where  $m_{\mathcal{H}^*}$  is a  $2\pi$ -periodic function,

$$m_{\mathcal{H}^*}(\xi) = m_2(2\xi) m_0(\xi). \quad (2.17)$$

The coefficients  $\tilde{d}_k^j = \langle \mathcal{H}f, \psi_k^j \rangle$  may then be computed as

$$\langle \mathcal{H}f, \psi_k^j \rangle \approx 2^{j/2} \int \hat{f}(\xi) e^{ik2^j \xi} \overline{m_2(2^{j-1}\xi)} \overline{\hat{\phi}(2^{j-1}\xi)} d\xi \quad (2.18)$$

$$= \sum_{\ell} b_{2\ell-1} \int \hat{f}(\xi) e^{i(2k-\ell-1/2)2^{j-1}\xi} \overline{\hat{\phi}(2^{j-1}\xi)} d\xi \quad (2.19)$$

$$= \sum_{\ell} b_{2\ell-1} s_{2k-\ell+1/2}^{j-1}, \quad (2.20)$$

since the coefficients  $b_{2\ell+1}$  are real.

Notice that as a consequence of equation (2.20), we now need “half-integer samples” of the coefficients  $s^{j-1}$ . In view of equation (2.16), this may be interpreted as follows. The shift by  $1/2$  actually amounts to a switch from  $\mathbf{V}_j$  to  $\mathbf{V}_{j-1}$ , as suggested by the following lemma:

**Lemma II.1** *Let  $f(x) \in \mathbf{V}_0$  or  $f(x) \in \mathbf{W}_0$ , and set  $f_{\frac{1}{2}}(x) = f(x + \frac{1}{2})$ . Then  $f_{\frac{1}{2}}(x) \in \mathbf{V}_{-1}$ .*

The proof of Lemma II.1 is very simple. Observe that  $f(x) \in \mathbf{V}_0$  is equivalent to  $\hat{f}(\xi) = q(\xi) \hat{\phi}(\xi)$ , where  $q(\xi)$  is a  $2\pi$ -periodic square-integrable function, and that translation by  $1/2$  is equivalent to multiplication by  $\exp\{i\xi/2\}$  in the Fourier space, so that  $\hat{f}_{\frac{1}{2}}(\xi) = \exp\{i\xi/2\} m_0(\xi/2) \hat{\phi}(\xi/2)$  which, in turn, implies that  $f_{\frac{1}{2}}(x) \in \mathbf{V}_{-1}$ . The argument for  $\mathbf{W}_0$  is the same.

From Lemma II.1 follows a simple algorithm to compute (2.20). In order to obtain “half-integer samples” on all scales except the finest scale  $j = 0$ , it is simply sufficient to avoid subsampling at the first step of the algorithm<sup>1</sup>.

At scale  $j = 0$ , we need to use interpolation to obtain “half-integer samples”  $s_{k+1/2}^0$ , using the assumption that  $f \in \mathbf{V}_0$ . We have

$$s_{k+1/2}^0 = \langle f, \phi_{k+1/2}^0 \rangle = \sum_{\ell} s_{\ell}^0 \langle \phi_{\ell}^0, \phi_{k+1/2}^0 \rangle, \quad (2.21)$$

where coefficients  $\langle \phi_{\ell}^0, \phi_{k+1/2}^0 \rangle$  are easily obtained using autocorrelation function of scaling function described in Appendix.

Summarizing, we obtain the following  $O(N)$  scheme for computing the coefficients  $\tilde{s}_k^j$  of the Hilbert transform of a function  $f(x)$  on subspace  $\mathbf{V}_j, j \geq 0$ , assuming that projection of  $f(x)$  onto an approximation space, say  $\mathbf{V}_0$  is known.

1. Compute the coefficients  $s_k^j, j \geq 1$  and  $k \in \mathbb{Z}/2$  using equation (9.9) in Appendix and the Hilbert differences  $\tilde{d}_k^j = \langle \mathcal{H}f, \psi_k^j \rangle$  via the pyramidal algorithm given in equation (2.20) on all scales.
2. Use the usual filters for the reconstruction on all scales: replace equation (9.10) by the following

$$\tilde{s}_k^j = \sum_{\ell} \left( h_{2\ell-k} \tilde{s}_{\ell}^{j+1} + g_{2\ell-k} \tilde{d}_{\ell}^{j+1} \right) \quad (2.22)$$

---

<sup>1</sup>Notice that in the particular case of the Hilbert transform, we would then use the even (non-sampled) scaling function coefficients to compute the difference coefficients  $d_k^j$ , and the odd ones for the Hilbert transform coefficients  $\tilde{d}_k^j$ .

We note that the computational cost is a factor of two compared with the usual wavelet transform.

**Remark:** Recently Auscher [1] and, independently, Lemarié [11] have shown (as a part of a more general result) that given a Multiresolution Analysis (MRA), it is possible to associate another MRA with the Hilbert transform of the associated wavelet  $\psi(x)$ . We notice that our construction is different in the sense that we never need to consider the scaling function associated with the new MRA. Also, we always derive approximate formulas since our goal is to develop efficient approximations suitable for numerical implementations.

### III IMPLEMENTATION OF OPERATORS VIA FILTER BANKS

Let us now turn to the more general case of filter bank implementation of linear operators. We show that the approach we developed for the Hilbert transform may be generalized to convolution operators with non-oscillatory kernels. We also analyze the connection with the BCR approach [3] and express the filter bank implementation as an approximation (with controlled accuracy) to the non-standard and standard forms (NS-form and S-form) approaches of [3], where we take into account only a few blocks of corresponding representations.

#### III.1 Convolution operators

Let us consider a more general convolution operator with symbol  $a(\xi)$ ,

$$\hat{g}(\xi) = a(\xi)\hat{f}(\xi), \quad (3.1)$$

and compute coefficients  $\tilde{d}_k^j$  of the projection of  $g$  on  $\mathbf{W}_j$ ,

$$\tilde{d}_k^j = \int g(x)\psi_k^j(x)dx = \frac{2^{j/2}}{2\pi} \int \hat{g}(\xi) \overline{\hat{\psi}(2^j\xi)} e^{ik2^j\xi} d\xi. \quad (3.2)$$

We look for the coefficients  $\tilde{b}_l^j$  such that

$$\tilde{d}_k^j \approx \sum_{\nu} \tilde{b}_{\nu}^j s_{\nu+2k}^{j-1}, \quad (3.3)$$

where

$$s_{\nu}^{j-1} = \frac{2^{(j-1)/2}}{2\pi} \int \hat{f}(\xi) \overline{\hat{\phi}(2^{j-1}\xi)} e^{i\nu 2^{j-1}\xi} d\xi, \quad (3.4)$$

and index  $\nu$  is not necessarily an integer. Typically, we will set  $\nu$  to be half-integer and, if more precision is needed, we will demonstrate that  $\nu$  can be taken to be in  $2^{-N}\mathbb{Z}$ . Using (3.1), we write (3.2) as

$$\tilde{d}_k^j = \frac{2^{j/2}}{2\pi} \int a(\xi) \hat{f}(\xi) \overline{m_1(2^{j-1}\xi)} \overline{\hat{\phi}(2^{j-1}\xi)} e^{ik2^j\xi} d\xi, \quad (3.5)$$

and note that it is sufficient to find an approximation

$$a(\xi) \overline{m_1(2^{j-1}\xi)} \overline{\hat{\phi}(2^{j-1}\xi)} e^{ik2^j\xi} \approx 2^{-1/2} \sum_{\nu} \tilde{b}_{\nu-2k}^j \overline{\hat{\phi}(2^{j-1}\xi)} e^{i\nu 2^{j-1}\xi}, \quad (3.6)$$

or

$$a(\xi) \overline{m_1(2^{j-1}\xi)} \approx 2^{-1/2} \sum_{\nu} \tilde{b}_{\nu}^j e^{i\nu 2^{j-1}\xi}. \quad (3.7)$$

over the essential support of the function  $\hat{\phi}(2^{j-1}\xi)$ . Let us replace  $2^{j-1}\xi$  by  $\xi$  in (3.7) and approximate  $a(2^{-j+1}\xi) \overline{m_1(\xi)}$  by the following  $4\pi$ -periodic function (i.e., restrict  $\nu$  to half integers,  $\nu = n/2$ )

$$\overline{m_{\#}^j(\xi)} = \sum_k a(2^{-j+1}(\xi + 4\pi k)) \overline{m_1(\xi + 4\pi k)} \chi_{[-2\pi, 2\pi]}(\xi + 4\pi k). \quad (3.8)$$

Due to  $M-1$  vanishing derivatives of  $m_1(\xi)$  at points  $2\pi k$ ,  $k \in \mathbb{Z}$ , at these points the ‘‘break’’ in the function due to the periodization occurs only in the higher derivatives. Since derivatives of  $m_1(\xi)$  vanish at  $\xi = 0$ , we can consider symbols that have a singularity at  $\xi = 0$ , *e.g.*, the Hilbert transform and fractional derivatives.

The Fourier coefficients of  $m_{\#}^j$  may be found by computing

$$b_n^j = \frac{\sqrt{2}}{4\pi} \int_{-2\pi}^{2\pi} \overline{a(2^{-j+1}\xi)} m_1(\xi) e^{-in\xi/2} d\xi, \quad (3.9)$$

since they are related to the  $\tilde{b}_{\nu}^j$  coefficients by a complex conjugation and a redefinition of the index  $\nu$ , and we have

$$m_{\#}^j(\xi) = \frac{1}{\sqrt{2}} \sum_n b_n^j e^{in\xi/2}. \quad (3.10)$$

The coefficients  $b_n^j$  have a fast asymptotic decay. Let us consider two cases, first where the symbol  $a(\xi)$  has at least  $M$  continuous derivatives ( $M$  is the number of vanishing moments of the basis) and, second, where  $a(\xi)$  has a singularity at  $\xi = 0$  but has at least  $M$  continuous derivatives elsewhere. In the first case we simply integrate (3.9) by parts  $M - 1$  times using

$$\left(\frac{2i}{n}\right)^m \frac{d^m}{d\xi^m} e^{-in\xi/2} = e^{-in\xi/2}, \quad (3.11)$$

and notice that the boundary terms vanish so that

$$b_n^j = O(n^{-M+1}). \quad (3.12)$$

In the second case we split the integral into two over  $[-2\pi, 0]$  and  $[0, 2\pi]$ , and then integrate by parts to obtain again (3.12).

Summarizing the results of this section, we show that the action of a convolution operator  $T$  with symbol  $a(\xi)$  on a function  $f(x)$  may be obtained as follows:

$$Tf(x) = \sum_j \sum_k \tilde{d}_k^j \psi_k^j(x) = \sum_j \sum_k \sum_n \overline{b_n^j} s_{2k-n/2}^{j-1} \psi_k^j(x) \quad (3.13)$$

where the coefficients  $b_n^j$  are given in (3.9). This implies that in order to evaluate  $T$  in the wavelet basis, we compute

$$\tilde{d}_k^j = \sum_n \overline{b_n^j} s_{2k-n/2}^{j-1} \quad (3.14)$$

Again, we notice that ‘‘half-integer samples’’ of the coefficients  $s^{j-1}$  are needed, and refer to the discussion in Section II.

The filter  $B_j = \{b_n^j\}$  defined in (3.9) may be used similar to the filter  $G$  in QMF pair. Namely, a signal  $f$  is decomposed using the filter pair  $H$  and  $B_j$  and then reconstructed with the usual QMF pair  $H$  and  $G$  to yield the desired result. Notice that the filters  $B_j$  depend on the scale. If the symbol  $a(\xi)$  is homogeneous of degree  $m$ , then  $b_n^j = 2^{-jm} b_n^0$ .

**Remark:** It is easy to see the similarities with the decomposition into a biorthogonal basis. We note, however, that there is a single MRA in our approach.

### III.2 Time-dependent symbols

A number of interesting questions arises if we consider a more general class of symbols of pseudodifferential operators,

$$\mathcal{T}_{\sigma} f(x) = \frac{1}{2\pi} \int_{\mathbb{R}} \sigma(\xi, x) \hat{f}(\xi) e^{i\xi x} d\xi, \quad (3.15)$$

where symbol  $\sigma(\xi, x) \in \mathcal{S}'(\mathbb{R}^2)$ . The operator  $\mathcal{T}_\sigma$  may be expressed as an integral operator of the form

$$\mathcal{T}_\sigma f(x) = \int_{\mathbb{R}} K(x, y) f(y) dy . \quad (3.16)$$

Here  $K(x, y) \in \mathcal{S}'(\mathbb{R}^2)$  is the distribution kernel of  $\mathcal{T}_\sigma$ , given by

$$K(x, y) = \left[ \mathcal{F}_1^{-1} \sigma \right] (x - y, x) = L(x - y, x) , \quad (3.17)$$

where  $\mathcal{F}_1$  denotes Fourier transform with respect to the first variable. To develop our approach, we need to specify further the symbol class we are working with. We restrict to the class of the so-called *Calderón-Zygmund kernels*, i.e. kernels  $K(x, y)$  such that

$$\left| \partial_x^\alpha \partial_y^\beta K(x, y) \right| \leq \frac{C_{\alpha, \beta}}{|x - y|^{1 + \alpha + \beta}} .$$

Let  $f(x) \in L^2(\mathbb{R})$ , and let us compute the projection of  $\mathcal{T}_\sigma f$  onto  $\mathbf{W}_j$ ,

$$\langle \mathcal{T}_\sigma f, \psi_k^j \rangle = 2^{-j/2} \int_{\mathbb{R} \times \mathbb{R}} L(x - y, x) f(y) \psi(2^{-j}x - k) dx dy \quad (3.18)$$

Let us focus on the integral with respect to  $x$  first. We write

$$\int L(x - y, x) f(y) \psi(2^{-j}x - k) dx = \int L(x - y, k2^j) \psi(2^{-j}x - k) dx + R(y; j, k) \quad (3.19)$$

where  $R(y; j, k)$  is some remainder. It follows from general arguments involving the vanishing moments of  $\psi(x)$  that

$$|R(y; j, k)| = O\left(2^{M(j-1/2)}\right) .$$

From now on, we assume that the remainder may be neglected, i.e., that we are at a sufficiently fine scale. Assuming that we may change the order of summation in (3.18), we arrive at an approximation

$$\langle \mathcal{T}_\sigma f, \psi_k^j \rangle \approx \frac{1}{2\pi} \int \sigma(\xi, k2^j) \hat{f}(\xi) e^{ik2^j\xi} \overline{m_1(2^{j-1}\xi)} \overline{\hat{\phi}(2^{j-1}\xi)} d\xi . \quad (3.20)$$

Repeating considerations of Section III.1, we construct the  $4\pi$ -periodic function

$$m_\sigma(\xi; k, j) = \sum_{n \in \mathbb{Z}} m_1(\xi + 4\pi n) \overline{\sigma(2^{-j+1}(\xi + 4\pi n), k2^j)} \chi_{[-2\pi, 2\pi]}(\xi + 4\pi n) . \quad (3.21)$$

Setting

$$m_\sigma(\xi; k, j) = \frac{1}{\sqrt{2}} \sum_{\ell} b_{k, \ell}^j e^{i\ell\xi/2} , \quad (3.22)$$

we obtain the Fourier coefficients of  $m_\sigma(\xi; k, j)$

$$b_{k, \ell}^j = \sum_n g_n \frac{1}{4\pi} \int_{-2\pi}^{2\pi} \overline{\sigma(2^{-j+1}\xi, k2^j)} e^{i(n-\ell/2)\xi} d\xi . \quad (3.23)$$

It is clear that the coefficients  $b_{k, \ell}^j$  have the expected asymptotic behavior as  $\ell \rightarrow \infty$ ,

$$b_{k, \ell}^j = O\left(\ell^{-L-1}\right) . \quad (3.24)$$

Finally, we obtain the following algorithm for computing the wavelet coefficients in (3.18),

$$\langle \mathcal{T}_\sigma f, \psi_k^j \rangle = \sum_{\ell} \overline{b_{k, \ell}^j} s_{\ell}^{j-1} . \quad (3.25)$$

This expression is similar to (3.14), except that the sum is no longer a convolution. Thus, strictly speaking, the algorithm in (3.25) is not a filter bank, since filter bank algorithms are usually understood to consist of convolutions.

### III.3 Connection with BCR approach

It is reasonable to expect that a subclass of Calderón-Zygmund operators (see *e.g.*, vol. 2 of [16]) may be implemented numerically via filter banks. Let us consider the class of symbols  $S_{1,1}^0$ , where  $\sigma \in S_{1,1}^0$  satisfies

$$|\partial_\xi^\alpha \partial_x^\beta \sigma(\xi, x)| \leq C(\alpha, \beta)(1 + |\xi|)^{\beta - \alpha} . \quad (3.26)$$

It was shown in [3] that in wavelet bases operators of this class may be represented by sparse matrices. All information is contained in the following set of coefficients

$$\begin{cases} \alpha_{k\ell}^j &= \langle T\psi_k^j, \psi_\ell^j \rangle \\ \beta_{k\ell}^j &= \langle T\phi_k^j, \psi_\ell^j \rangle \\ \gamma_{k\ell}^j &= \langle T\psi_k^j, \phi_\ell^j \rangle , \end{cases} \quad (3.27)$$

which gives rise to the “NS-form”, an alternative to the “S-form” consisting of the elements  $\langle T\psi_k^j, \psi_{k'}^j \rangle$  (see [3] for more details).

To explain the relation of the filter bank approach to that using NS-form, let us consider wavelets with good localization in the Fourier domain (*e.g.*, Battle-Lemarié wavelets), so that for a given precision we need to consider “interaction” between scales which are immediate neighbors. In this case we may consider the simplified S-form where only interaction between neighboring scales is taken into account. Thus, for a given subspace  $\mathbf{W}_j$ , only its mappings from subspaces  $\mathbf{W}_{j+1}$ ,  $\mathbf{W}_j$  and  $\mathbf{W}_{j-1}$  are significant, and these are subspaces of  $\mathbf{V}_{j-2}$ . In this approximation we then consider the mapping  $\mathbf{V}_{j-2} \rightarrow \mathbf{W}_j$  which is exactly the one considered in

$$\widehat{T\psi}(\xi) = m_T(\xi/4)\hat{\phi}(\xi/4) , \quad (3.28)$$

where

$$m_T(\xi) = m_\#(2\xi)m_0(\xi) \quad (3.29)$$

and  $m_\#$  is defined in (3.8) (we suppress the scale index  $j$ ).

If more accuracy is required, one may consider mappings between more scales, *e.g.*,  $\mathbf{W}_{j+2}$ ,  $\mathbf{W}_{j+1}$ ,  $\mathbf{W}_j$ ,  $\mathbf{W}_{j-1}$  and  $\mathbf{W}_{j-2}$ , which amounts to considering the mapping  $\mathbf{V}_{j-3} \rightarrow \mathbf{W}_j$ . This corresponds to an approximation

$$\widehat{T\psi}(\xi) = \tilde{m}_T(\xi/8)\hat{\phi}(\xi/8) , \quad (3.30)$$

where

$$\tilde{m}_T(\xi) = \tilde{m}_\#(4\xi)m_0(2\xi)m_0(\xi) \quad (3.31)$$

and  $\tilde{m}_\#$  is defined similar to  $m_\#$ , except that the  $4\pi$ -periodization in (3.8) is replaced with the  $8\pi$ -periodization.

Let us then consider again a convolution operator  $T$  with symbol  $a(\xi)$ . Following [3], we consider

$$P_0TP_0 = P_JTP_J + \sum_{j=1}^J [Q_jTQ_j + Q_jTP_j + P_jTQ_j] \quad (3.32)$$

$$= P_JTP_J + \sum_{j=1}^J [Q_jTP_{j-1} + P_jTQ_j] . \quad (3.33)$$

The action of first term  $Q_j T P_{j-1}$  on  $f(x) \in \mathbf{L}^2(\mathbb{R})$  (putting together  $P_j$  and  $Q_j$  is motivated by Lemma II.1) may be evaluated with the same type of approximation as discussed before,

$$Q_j T P_{j-1} f(x) = \sum_{k,\ell} s_\ell^{j-1} \langle \phi_\ell^{j-1}, T^* \psi_k^j \rangle \psi_k^j(x) . \quad (3.34)$$

Using notation of the previous section, we have

$$\langle T \phi_\ell^{j-1}, \psi_k^j \rangle = \frac{1}{2\pi} 2^{j-1/2} \int e^{i(2k-\ell)2^{j-1}\xi} a(\xi) \overline{m_1(2^{j-1}\xi)} \left| \hat{\phi}(2^{j-1}\xi) \right|^2 d\xi \quad (3.35)$$

$$\approx \frac{1}{2\pi} 2^{j-1/2} \int e^{i(2k-\ell)2^{j-1}\xi} \overline{m_{\#}^j(2^{j-1}\xi)} \left| \hat{\phi}(2^{j-1}\xi) \right|^2 d\xi \quad (3.36)$$

$$= \sum_n \overline{b_n^j} \frac{1}{2\pi} \int e^{i(2k-\ell-n/2)\xi} \left| \hat{\phi}(\xi) \right|^2 d\xi . \quad (3.37)$$

Finally, using the definition of coefficients  $a_{2\ell-1}$  in Appendix, we obtain for the coefficient of  $\psi_k^j(x)$  in (3.34),

$$\sum_\ell \langle T \phi_\ell^{j-1}, \psi_k^j \rangle s_\ell^{j-1} = \sum_\ell \overline{b_{2(2k-\ell)}^j} s_\ell^{j-1} + \frac{1}{2} \sum_{\ell,n} a_{2n-1} \left( \overline{b_{2(2\ell-k)+(2n-1)}^j} + \overline{b_{2(2\ell-k)-(2n-1)}^j} \right) s_\ell^{j-1} . \quad (3.38)$$

Comparing this expression with equation (3.13) and interchanging the order of summation, we recognize here the same structure as that described in Section III.1. We may interpret the summation in (3.38) as interpolation to obtain the half-integer translates coefficients  $s_k^{j-1}$ . Coefficients  $b_k$  are given in (3.9).

Let us now turn to the  $P_j T Q_j$  term. We notice that in order to describe this term, it is sufficient consider only  $Q_{j+1} T Q_j$ ,

$$P_j T Q_j f \approx Q_{j+1} T Q_j f ,$$

due to considerations above. This term represents mapping from scale  $j$  to scale  $j+1$ , and

$$Q_{j+1} T Q_j f(x) = \sum_{k,\ell} d_k^j \langle T \psi_k^j, \psi_\ell^{j+1} \rangle \psi_\ell^{j+1}(x) = \sum_\ell q_\ell^j \psi_\ell^{j+1}(x) . \quad (3.39)$$

As before, we approximate the coefficient  $\omega_{k-2\ell}^j = \langle T \psi_k^j, \psi_\ell^{j+1} \rangle$  as follows

$$\begin{aligned} \omega_{k-2\ell}^j &= \frac{1}{2\pi} 2^{j+1/2} \int e^{i(2\ell-k)2^j\xi} a(\xi) \overline{m_0(2^{j-1}\xi)} \overline{m_1(2^j\xi)} m_1(2^{j-1}\xi) \left| \hat{\phi}(2^{j-1}\xi) \right|^2 d\xi \\ &\approx \frac{1}{2\pi} 2^{j+1/2} \int e^{i(4\ell-2k)2^{j-1}\xi} a(\xi) \overline{m_{\#}^{j+1}(2^j\xi)} \overline{m_0(2^{j-1}\xi)} m_1(2^{j-1}\xi) \left| \hat{\phi}(2^{j-1}\xi) \right|^2 d\xi \\ &\approx \sum_n \overline{b_n^{j+1}} c_{n+2k-4\ell} , \end{aligned} \quad (3.40)$$

where we have set for simplicity

$$\overline{m_0(\xi)} m_1(\xi) = \frac{1}{2} \sum_n c_n e^{in\xi} . \quad (3.41)$$

Again, we obtain for the coefficients  $q_\ell^j$  in (3.39) a filter bank type relation,

$$q_\ell^j = \sum_k \omega_{k-2\ell}^j d_k^j . \quad (3.42)$$

The results of this section may be summarized as follows. From equations (3.13), (3.38) and (3.42) we have

$$\begin{aligned}
\tilde{d}_k^j &= \sum_n \overline{b_n^j} s_{2k-n/2}^{j-1} \\
&= \sum_\ell \overline{b_{2(2k-\ell)}^j} s_\ell^{j-1} + \frac{1}{2} \sum_{\ell,n} a_{2n-1} \left( \overline{b_{2(2\ell-k)+(2n-1)}^j} + \overline{b_{2(2\ell-k)-(2n-1)}^j} \right) s_\ell^{j-1} \\
&\quad + \sum_k \omega_{k-2\ell}^{j-1} d_k^{j-1},
\end{aligned} \tag{3.43}$$

which is a filter bank type representation obtained using elements of the NS-form. The terms in (3.43) may be interpreted as follows: the first two terms of the r.h.s. of (3.43) may be viewed as representing the “half-integer samples” discussed in Section II via interpolation within  $\mathbf{V}_{j-1}$  and the third term is an element of  $\mathbf{W}_{j-1}$  so that (3.43) represents the mapping  $\mathbf{V}_{j-2} \rightarrow \mathbf{W}_j$ .

## IV HILBERT TRANSFORM OF AUTOCORRELATION WAVELETS

In Section II we have described an approximation of the action of the Hilbert transform on wavelets. These approximate filters have to be applied to the coefficients of the function on subspaces  $\mathbf{V}_j$ . Since the discrete Hilbert transform is usually defined directly on the samples of the function, it is advantageous to require that the coefficients  $s_k^j$  are (at least approximately) the values of the function. This requirement may be satisfied by considering interpolating scaling functions. Examples of such scaling functions proposed in [19] are obtained as autocorrelations of the usual compactly supported scaling functions. The properties of such autocorrelation wavelets and scaling functions are described in Appendix. We note that by using symmetric interpolating wavelets in this section, we give up orthogonality of the basis.

In view of the applications we consider further in the paper, we will elaborate on the case of the so-called dyadic wavelet transform (which is redundant with respect to the translation variable, see Appendix). As a result we obtain an  $O(N \log N)$  algorithm for decomposition and computing the Hilbert transform. Let us make clear that the redundancy may be avoided (yielding an  $O(N)$  algorithm) if we follow considerations of Section II.

### IV.1 Representation of the Hilbert transform

Let us consider

$$\tilde{m}_1(\xi) = i \operatorname{sgn}(\xi) |m_1(\xi)|^2 \quad (4.1)$$

and denote by  $\tilde{m}_1^c(\xi)$  its restriction to the interval  $[-2\pi, 2\pi]$ . Let

$$m_2(\xi) = \sum_{k=-\infty}^{\infty} \tilde{m}_1^c(\xi + 4\pi k), \quad (4.2)$$

and consider its Fourier series,

$$m_2(\xi) = 2i \sum_{k=1}^{\infty} b_k \sin\left(\frac{k\xi}{2}\right), \quad (4.3)$$

where  $m_2$  is a  $4\pi$ -periodic function. The adverse effect of the restriction to  $[-2\pi, 2\pi]$  and of the  $4\pi$ -periodization in (4.2) is weakened by the fact that the problematic point in multiplying by  $i \operatorname{sgn}(\xi)$  is at the origin  $\xi = 0$ , where  $m_1$  has a zero of order  $L$ . Therefore, the sequence  $b_k$  in (4.3) has fast decay and, since  $\hat{\Phi}(\xi)$  is concentrated around  $\xi = 0$ , we may expect the product  $m_2(\xi)\hat{\Phi}(\xi)$  to be a good approximation for  $\operatorname{sgn}(\xi)|m_1(\xi)|^2\hat{\Phi}(\xi)$ . Let  $\tilde{T}_j f = T_j(\mathcal{H}f)$  denote the  $j$ th scale of dyadic wavelet transform of the Hilbert transform of  $f$ . We prove

**Theorem IV.1** *Let  $\Psi$  be the autocorrelation of the Daubechies' compactly supported wavelet with  $L/2$  vanishing moments. Then the coefficients of  $\tilde{T}_j f = T_j(\mathcal{H}f)$  may be approximated by those obtained from the following pyramidal algorithm:*

$$W_j f(n) = \sum_{k=1}^{\infty} b_{2k-1} [S_j f(n + k2^{j-1} - 2^{j-2}) - S_j f(n - k2^{j-1} + 2^{j-2})], \quad (4.4)$$

where the sequence  $b_k$  is given by

$$b_k = \begin{cases} 0, & \text{for } k = 2m, \\ \frac{-1}{(2m-1)\pi} \left[ 1 - \sum_{\ell=1}^{L/2} a_{2\ell-1} \frac{1}{1 - 4\left(\frac{2\ell-1}{2m-1}\right)^2} \right], & \text{for } k = 2m-1, \end{cases} \quad (4.5)$$

and decays at infinity as

$$b_{2k-1} = O((2k-1)^{-L-1}) . \quad (4.6)$$

In addition, the exact and approximate Hilbert transform coefficients satisfy

$$\|\tilde{T}_j f - W_j f\| \leq 2K^2(1+2\pi)^{-2\alpha L} \|f\| , \quad (4.7)$$

where  $\alpha$  is the Hölder regularity of the scaling function  $\phi(x)$ .

The theorem is proved below, and the proof follows the lines of that of Proposition II.1. We detail it for completeness.

#### IV.1.1 Computation of coefficients $b_{2k-1}$ and their behavior for large $k$

We have

$$\begin{aligned} b_k &= \frac{1}{2\pi} \frac{1}{2i} \int_{-2\pi}^{2\pi} i \operatorname{sgn}(\xi) \sin\left(\frac{k\xi}{2}\right) |m_1(\xi)|^2 d\xi \\ &= \frac{1}{8\pi} \int_{-2\pi}^{2\pi} \sin\left(\frac{k\xi}{2}\right) \operatorname{sgn}(\xi) d\xi \\ &\quad - \frac{1}{8\pi} \sum_{\ell=1}^{L/2} a_{2\ell-1} \int_{-2\pi}^{2\pi} \sin\left(\frac{k\xi}{2}\right) \cos((2\ell-1)\xi) \operatorname{sgn}(\xi) d\xi . \end{aligned} \quad (4.8)$$

The computation of the integrals in (4.8) yields (4.5).

If  $k$  is large enough,  $2k-1 > 2(2\ell-1)$ , then  $\frac{1}{1-4\left(\frac{2\ell-1}{2k-1}\right)^2}$  may be replaced by its Taylor series, namely,

$$\frac{1}{1-4\left(\frac{2\ell-1}{2k-1}\right)^2} = \sum_{p=0}^{\infty} \left(2\frac{2\ell-1}{2k-1}\right)^{2p} \quad (4.9)$$

According to Lemma IX.2 of Appendix, the sequence  $\{a_{2\ell-1}\}$  has  $L-1$  vanishing even moments, and we have

$$\begin{aligned} b_{2k-1} &= \frac{-1}{\pi(2k-1)} 2 \sum_{p=L}^{\infty} (2k-1)^{-2p} \sum_{\ell=1}^{L/2} a_{2\ell-1} 2^{2p} (2\ell-1)^{2p} \\ &= \frac{-1}{\pi} (2k-1)^{-L-1} \sum_{\ell=1}^{L/2} a_{2\ell-1} \frac{[2(2\ell-1)]^L}{1 - \left(2\frac{2\ell-1}{2k-1}\right)^2} \\ &= O((2k-1)^{-L-1}) . \end{aligned} \quad (4.10)$$

#### IV.1.2 Pyramidal algorithm

Let us consider the approximate wavelet transform of  $\mathcal{H}f$ ,

$$\begin{aligned} W_j f(n+w) &= \frac{1}{2\pi} \int_{-\infty}^{\infty} \hat{f}(\xi) e^{i\xi(n+w)} \overline{m_2(2^{j-1}\xi)} \overline{\widehat{\Phi}(2^{j-1}\xi)} d\xi \\ &= \sum_{k=1}^{\infty} b_{2k-1} [S_{j-1} f(n+w+k2^{j-1}-2^{j-2}) - S_{j-1} f(n+w-k2^{j-1}+2^{j-2})] . \end{aligned} \quad (4.11)$$

By setting  $w=0$ , we arrive at (4.4).

**Remarks:**

1. As in the orthogonal case, we note that for  $j = 1$  (and only in this case, since we are now using the dyadic wavelet transform) we need samples of  $S_0 f$  for half-integer  $n$ . Thus, an additional interpolation procedure is required for the first step of the algorithm,  $j = 1$ . An alternative is to set  $w = 2^{j-2}$ , which would yield half integer samples of the Hilbert transform coefficients. We will come back to this point later on.
2. In order to compute the wavelet coefficients of  $f(x)$  with respect to the Hilbert transform of  $\Psi(x)$ , we just need to use (4.4), since  $\langle f, \mathcal{H}\Psi_{jk} \rangle = -\langle \mathcal{H}f, \Psi_{jk} \rangle$ .

**IV.1.3 Accuracy estimate**

Let us introduce the following function

$$\widehat{\Theta}(\xi) = m_2\left(\frac{\xi}{2}\right)\widehat{\Phi}\left(\frac{\xi}{2}\right) \approx \widehat{\mathcal{H}^*\Psi}(\xi) \tag{4.12}$$

where  $m_2$  is the  $4\pi$ -periodic function given in equation (4.2). The function  $\Theta$  is also a wavelet, and has, in fact, the same number of vanishing moments as  $\Psi$ .

Considering  $f \in L^2(\mathbb{R})$ , we fix  $j$  and compute

$$\|\widetilde{T}_j f - W_j f\|^2 \leq \|\widehat{\Theta}_j - \widehat{\mathcal{H}\Psi}_j\|_\infty^2 \|f\|^2, \tag{4.13}$$

and

$$|\widehat{\Theta}_j(\xi) - \widehat{\mathcal{H}\Psi}_j(\xi)|^2 = |m_2(2^{j-1}\xi) - \widetilde{m}_1(2^{j-1}\xi)|^2 |\widehat{\phi}(2^{j-1}\xi)|^4. \tag{4.14}$$

Since we know that for some positive  $K$  [5]

$$|\widehat{\phi}(\xi)| \leq K[1 + |\xi|]^{-\alpha L}, \tag{4.15}$$

and that  $m_2 - \widetilde{m}_1 = 0$  inside the interval  $[-2\pi, 2\pi]$ , it follows that

$$\|\widehat{\Theta}_j - \widehat{\mathcal{H}\Psi}_j\|_\infty^2 \leq 4K^4(1 + 2\pi)^{-4\alpha L}. \tag{4.16}$$

This completes the proof of Theorem (IV.1).

**IV.2 Numerical examples**

The coefficients  $b_{2k-1}$  are easy to compute numerically using equation (4.5). We present in Figure 1 a plot of the approximate filter  $m_2(\xi)$  (up to a factor  $i$ ) for the case of the autocorrelation of Daubechies' wavelet with 5 vanishing moments. As expected, we observe the sign flip in  $[-2\pi, 0]$ .

We also provide tables of the twenty top coefficients  $b_{2k-1}$  in (4.5) for the autocorrelation of Daubechies' compactly supported wavelets with  $L = 2, 4, 6, \dots, 12$  (the numerical values of the  $a_{2\ell-1}$  coefficients are listed in [2]). The coefficients  $b_{2k-1}$  have been computed using Mathematica™.

n	$L = 2$	$L = 4$	$L = 6$
1	0.4244131815783876	0.4365392724806273	0.4409487600814417
2	-0.0848826363156775	-0.1131768484209033	-0.1243701630998938
3	-0.01212609090223965	-0.03968538840732975	-0.052913851209773
4	-0.004042030300746545	0.01119331467899044	0.02194767584115772
5	-0.001837286500339341	0.001469829200271469	0.007735943159323537
6	-0.00098930811556734	0.0004190010842402825	-0.001995243258287072
7	-0.0005935848693404007	0.0001606695886936418	-0.000232854476367596
8	-0.0003840843272202589	0.00007315891947052786	-0.0000585271355764204
9	-0.000262794539677021	0.00003739368944020764	-0.00001978502086783541
10	-0.0001877103854835852	0.00002079253500741326	-7.96648850858781 . 10 <sup>-6</sup>
11	-0.0001387424588356934	0.0000123326630076163	-3.616616717774846 . 10 <sup>-6</sup>
12	-0.0001054442687151276	7.699784328080609 . 10 <sup>-6</sup>	-1.794821521695973 . 10 <sup>-6</sup>
13	-0.000082012209000655	5.012630770837775 . 10 <sup>-6</sup>	-9.54786813494256 . 10 <sup>-7</sup>
14	-0.00006504416575913947	3.378917701774295 . 10 <sup>-6</sup>	-5.371888238108361 . 10 <sup>-7</sup>
15	-0.00005245497238640281	2.345812429702546 . 10 <sup>-6</sup>	-3.165738771540177 . 10 <sup>-7</sup>
16	-0.00004291770467978535	1.670310668617303 . 10 <sup>-6</sup>	-1.939965933354726 . 10 <sup>-7</sup>
17	-0.00003556038387753632	1.215739619744941 . 10 <sup>-6</sup>	-1.229261496214611 . 10 <sup>-7</sup>
18	-0.00002979383514063819	9.02084159009443 . 10 <sup>-7</sup>	-8.01852585796044 . 10 <sup>-8</sup>
19	-0.00002521016819592433	6.808447524779539 . 10 <sup>-7</sup>	-5.365206875248337 . 10 <sup>-8</sup>
20	-0.00002152087528920315	5.2171818882981 . 10 <sup>-7</sup>	-3.671486198725726 . 10 <sup>-8</sup>

Table 1: Coefficients  $b_{2\ell-1}$  in (4.5), for  $L = 2$  to 6.

n	$L = 8$	$L = 10$	$L = 12$
1	0.4432100357741671	0.4445822030675855	0.4455026631153445
2	-0.130355892874755	-0.1340803469568908	-0.1366208166887056
3	-0.06064979436909654	-0.06572084740999089	-0.06930041426238691
4	0.0292635677882103	0.03447780350320051	0.03836151010471045
5	0.01318473790632533	0.01757965054176712	0.02111302943477737
6	-0.005214235714990194	-0.00832222843180702	-0.01109630457574269
7	-0.001690351013631451	-0.003533378893010262	-0.005429064711799898
8	0.0003955627094130471	0.001294568867169978	0.002419194330927688
9	0.000041697463334364	0.0003859993748666682	0.000958070243258808
10	$9.46322271323068 \cdot 10^{-6}$	$-0.0000828671394347809$	$-0.0003260788250929472$
11	$2.893293374219203 \cdot 10^{-6}$	$-8.01219703630296 \cdot 10^{-6}$	$-0.0000901837991993347$
12	$1.05641146622484 \cdot 10^{-6}$	$-1.669645439302717 \cdot 10^{-6}$	$0.00001795796428048217$
13	$4.362196164208865 \cdot 10^{-7}$	$-4.695520123574504 \cdot 10^{-7}$	$1.611795560157781 \cdot 10^{-6}$
14	$1.975403554736398 \cdot 10^{-7}$	$-1.580322843778648 \cdot 10^{-7}$	$3.121943903617391 \cdot 10^{-7}$
15	$9.61991936764573 \cdot 10^{-8}$	$-6.028730899715279 \cdot 10^{-8}$	$8.17340547747354 \cdot 10^{-8}$
16	$4.970370234553768 \cdot 10^{-8}$	$-2.528100401785013 \cdot 10^{-8}$	$2.565200407764876 \cdot 10^{-8}$
17	$2.698043149571869 \cdot 10^{-8}$	$-1.142700627907823 \cdot 10^{-8}$	$9.14160502347676 \cdot 10^{-9}$
18	$1.527338258524505 \cdot 10^{-8}$	$-5.492315158861647 \cdot 10^{-9}$	$3.587423126542339 \cdot 10^{-9}$
19	$8.96488105284584 \cdot 10^{-9}$	$-2.779542068231209 \cdot 10^{-9}$	$1.520111141096179 \cdot 10^{-9}$
20	$5.431028641232384 \cdot 10^{-9}$	$-1.470052866713106 \cdot 10^{-9}$	$6.86119176316265 \cdot 10^{-10}$

Table 2: Coefficients  $b_{2\ell-1}$  in (4.5), for  $L = 8$  to 12.

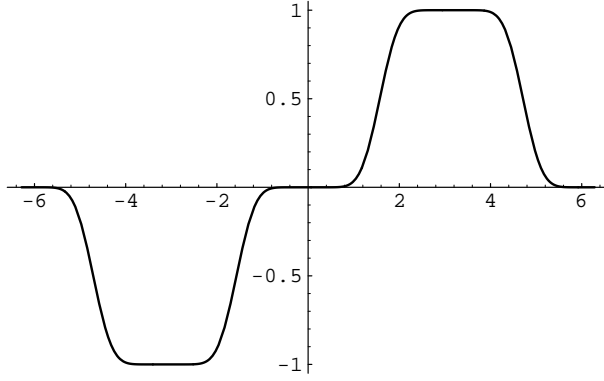


Figure 1: The  $4\pi$ -periodic function  $m_2(\xi)$  in (4.2), for the autocorrelation of Daubechies' wavelet with  $M = 5$ .

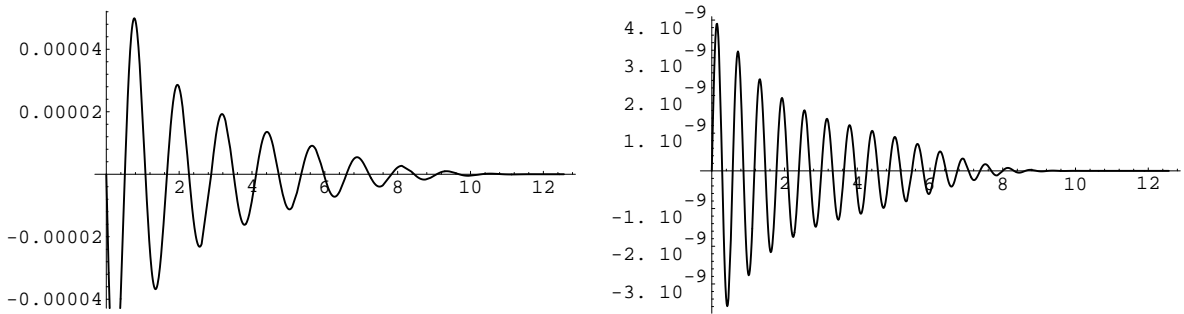


Figure 2: Error of the approximation  $\hat{\Theta}(\xi) - \hat{\Psi}(\xi)$  for the autocorrelation of Daubechies' wavelet with  $M = 2$  and  $M = 5$ .

To check numerically the accuracy of our approach, we compare  $\hat{\Theta}(\xi)$  and  $\hat{\Psi}(\xi)$  for positive values of  $\xi$ . The difference is plotted in Figure 2 for  $L = 2$  and  $L = 5$ , respectively. In both cases only the twenty top coefficients  $b_{2\ell-1}$  have been considered for the evaluation of  $m_2(\xi)$ .

Table 3 contains a numerical estimate for the absolute value of the error  $\max_{\xi \in [0, \pi]} |\hat{\Theta} - \hat{\Psi}|$ , computed for  $L = 2$  to  $L = 12$ .

### IV.3 Improving the accuracy

It is clear from the estimate (4.16) and examples in Figure 2 that the accuracy may be controlled by increasing the number of vanishing moments of wavelets. Also, the accuracy estimate may be improved by considering the restriction of  $\tilde{m}_1$  to a larger interval. Let  $\tilde{m}_1^c$  denote the restriction of  $\tilde{m}_1$  to the interval  $[-2^n\pi, 2^n\pi]$ , and set

$$m_2(\xi) = \sum_{k=-\infty}^{\infty} \tilde{m}_1^c(\xi + 2^n\pi k). \quad (4.17)$$

$L$	$\max  \hat{\Theta} - \hat{\Psi} $
2	0.004947346141230947
4	0.00004971880110332672
6	$1.100651917741455 \cdot 10^{-6}$
8	$1.677262504691843 \cdot 10^{-8}$
10	$3.903637503521736 \cdot 10^{-9}$
12	$1.112982483952842 \cdot 10^{-10}$

Table 3: Error  $\max_{\xi \in [0, \pi]} |\hat{\Theta} - \hat{\Psi}|$  as a function of the number of vanishing moments, for  $L = 2$  to 12.

Here  $m_2$  is a  $2^{n+1}\pi$ -periodic function. Let  $b_k$  denote the Fourier coefficients of  $m_2$ ,

$$\begin{aligned}
b_k &= \frac{1}{2^{n+2}\pi} \int_{-2^n\pi}^{2^n\pi} \sin(2^{-n}k\xi) \operatorname{sgn}(\xi) d\xi \\
&- \frac{1}{2^{n+2}\pi} \sum_{\ell=1}^{L/2} a_{2\ell-1} \int_{-2\pi}^{2\pi} \sin(2^{-n}k\xi) \cos((2\ell-1)\xi) \operatorname{sgn}(\xi) d\xi \quad .
\end{aligned} \tag{4.18}$$

The same computation as before yields

$$m_2(\xi) = 2i \sum_{k=1}^{\infty} b_{2k-1} \sin((2k-1)2^{-n}\xi), \tag{4.19}$$

where

$$b_{2k-1} = \frac{-1}{(2k-1)\pi} \left[ 1 - \sum_{\ell=1}^{L/2} a_{2\ell-1} \frac{1}{1 - 2^{2n} \left( \frac{2\ell-1}{2k-1} \right)^2} \right], \tag{4.20}$$

and

$$b_{2k-1} = O((2k-1)^{-L-1}) \tag{4.21}$$

for  $2k-1 > 2^n(2\ell-1)$ .

Let us consider the function  $\Theta$  defined by  $\hat{\Theta}(\xi) = m_2(\frac{\xi}{2})\hat{\Phi}(\frac{\xi}{2})$ . For  $f \in L^2(\mathbb{R})$  and fixed  $j$  we have

$$\begin{aligned}
W_j f(m) &= \frac{1}{2\pi} \int_{\infty}^{\infty} \hat{f}(\xi) e^{i\xi m} \overline{\hat{\Theta}(2^j \xi)} d\xi \\
&= \sum_{k=1}^{\infty} b_{2k-1} [S_{j-1} f(m + k2^{j-n} - 2^{j-n-1}) - S_{j-1} f(m - k2^{j-n} + 2^{j-n-1})] \quad .
\end{aligned} \tag{4.22}$$

The accuracy estimate is derived essentially as before. The only change is that  $2\pi$  has to be replaced by  $2^n\pi$ . We then obtain

$$\|\tilde{T}_j f - W_j f\|^2 \leq 4K^4 (1 + 2^n\pi)^{-4\alpha L} \|f\|^2, \tag{4.23}$$

as a generalization of (4.13) and (4.16).

## V OTHER EXAMPLES

A particularly simple implementation (similar to that for the Hilbert transform) is possible for the convolution operators with non-oscillatory kernel considered in [2]. The coefficients of filters (similar to  $m_2$ ) might be scale dependent. If the operator is homogeneous of some degree, then filters on different scales will differ only by a scaling factor.

This section is devoted to the study of the action of various operators of differentiation and integration including those of fractional order. Throughout the section, we will only use the autocorrelation wavelets that we used for the Hilbert transform, leaving to the reader the (straightforward) computations in the orthogonal case, as described in Section II.

### V.1 Derivative operators

The Hilbert transform is homogeneous of degree zero and, therefore, the operator (and, thus,  $m_2$ ) is the same on all scales. Since derivative operators are homogeneous, the filter will be the same on all scales except for a scaling factor,

$$\frac{d^n}{dx^n} \Psi_{jk} = 2^{-nj} \left( \frac{d^n \Psi}{dx^n} \right)_{jk}. \quad (5.1)$$

Thus, it is sufficient to evaluate the derivative operator on the function  $\psi$ . Our analysis is based on an approximation of  $\xi|m_1(\xi)|^2$  by the  $4\pi$ -periodization of its restriction to  $[-2\pi, 2\pi]$ . Let us consider (for simplicity) the case  $n = 1$ , and the  $4\pi$ -periodic function

$$m_3(\xi) = \sum_{k=-\infty}^{\infty} (\xi + 4\pi k) |m_1(\xi + 4\pi k)|^2 \chi_{[-2\pi, 2\pi]}(\xi + 4\pi k). \quad (5.2)$$

Since  $m_3$  is an odd function, we have

$$m_3(\xi) = \sum_{k=1}^{\infty} \delta_k \sin\left(\frac{k\xi}{2}\right). \quad (5.3)$$

An explicit computation of the Fourier coefficients  $\delta_k$  yields

$$\delta_k = \begin{cases} -\frac{2(-1)^k}{k} \left[ 1 - \sum_{\ell=1, \ell \neq \ell_0}^{L/2} a_{2\ell-1} \frac{1}{1 - \left(\frac{2(2\ell-1)}{k}\right)^2} \right] + \frac{1}{2k} a_{k/2} & \text{if } k = 2(2\ell_0 - 1) \\ -\frac{2(-1)^k}{k} \left[ 1 - \sum_{\ell=1}^{L/2} a_{2\ell-1} \frac{1}{1 - \left(\frac{2(2\ell-1)}{k}\right)^2} \right] & \text{otherwise.} \end{cases} \quad (5.4)$$

As in the case of the Hilbert transform, the behavior of the Fourier coefficients is governed by the number of vanishing moments of the wavelet. Using Lemma IX.2 and the Taylor series expansion of  $\delta_k$  for  $k > 2(2L - 1)$ , we estimate  $\delta_k$  as

$$\begin{aligned} \delta_k &= -2(-1)^k k^{-L-1} \sum_{\ell=1}^{L/2} a_{2\ell-1} \frac{(2(2\ell-1))^L}{1 - \left(\frac{2(2\ell-1)}{k}\right)^2} \\ &= O(k^{-L-1}) \end{aligned} \quad (5.5)$$

For a given precision, the series (5.5) may be truncated. As an example, we provide in Tables 4 and 5 coefficients  $\delta_k$  for the autocorrelation of the Daubechies wavelet with 4, 5 and 6 vanishing moments. The shape of filter  $m_3$  in the Fourier domain is shown in Figure 3.

n	$L = 8$	$L = 10$	$L = 12$
1	2.784770784770785	2.793392366147784	2.799175787195709
2	-0.67291259765625	-0.6661834716796875	-0.6615571975708008
3	-0.819050230814937	-0.842451665981078	-0.858413908073351
4	0.3888888888888888	0.4090909090909091	0.4230769230769232
5	-0.3810738968633705	-0.4129362628218463	-0.4354273446748881
6	0.08673095703125	0.0863571166992188	0.0855073928833008
7	0.1838684191625368	0.2166304283951343	0.2410324766511379
8	-0.0883838383838384	-0.1101398601398601	-0.1269230769230769
9	0.0828421514920371	0.1104562019893828	0.1326570763346433
10	-0.02213134765624998	-0.02583160400390625	-0.02801492214202881
11	-0.03276200923259743	-0.05229010340572205	-0.06972013787429609
12	0.0135975135975136	0.02447552447552448	0.034841628959276
13	-0.01062078865282526	-0.02220087434526055	-0.03411181962890829
14	0.003513881138392858	0.006190844944545201	0.00838465350014823
15	0.002485393803852205	0.00813401608533453	0.015200246275297
16	-0.0006798756798756801	-0.003239407651172366	-0.006876637294593952
17	0.0002619928889691353	0.002425305600742754	0.006019732875689713
18	-0.0001186794704861111	-0.00081475575764974	-0.001737650235493968
19	0.00005945918191033914	-0.0005206695929446174	-0.002048813682806388
20	-0.00003199414964121239	0.0001363961116283008	0.0007859014050964675
21	0.00001817909841825415	-0.00005034211869672657	-0.000566641522074894
22	-0.00001078904277146913	0.00002184781161221591	0.0001923626119440171
23	$6.637629002919957 \cdot 10^{-6}$	$-0.00001049069169242624$	$0.0001128332173139814$
24	$-4.209756531740421 \cdot 10^{-6}$	$5.412544112237683 \cdot 10^{-6}$	$-0.00002847468859045373$
25	$2.740848684599229 \cdot 10^{-6}$	$-2.95028230500094 \cdot 10^{-6}$	$0.00001012721018176066$

Table 4: Approximate coefficients  $\delta_k$  in (5.5) for the derivative of the autocorrelation wavelets with 4, 5 and 6 vanishing moments .

n	$L = 8$	$L = 10$	$L = 12$
26	$-1.825838007469143 \cdot 10^{-6}$	$1.680600893253589 \cdot 10^{-6}$	$-4.236514751727765 \cdot 10^{-6}$
27	$1.241182659087006 \cdot 10^{-6}$	$-9.92946127263026 \cdot 10^{-7}$	$1.961575206504767 \cdot 10^{-6}$
28	$-8.59133986072117 \cdot 10^{-7}$	$6.051291554033864 \cdot 10^{-7}$	$-9.76275037383496 \cdot 10^{-7}$
29	$6.044373602704397 \cdot 10^{-7}$	$-3.787963341003061 \cdot 10^{-7}$	$5.135502120568286 \cdot 10^{-7}$
30	$-4.31561710856343 \cdot 10^{-7}$	$2.427534623539174 \cdot 10^{-7}$	$-2.824343167784349 \cdot 10^{-7}$

Table 5: Approximate coefficients  $\delta_k$  in (5.5) for the derivative of the autocorrelation wavelets with 4, 5 and 6 vanishing moments (continued).

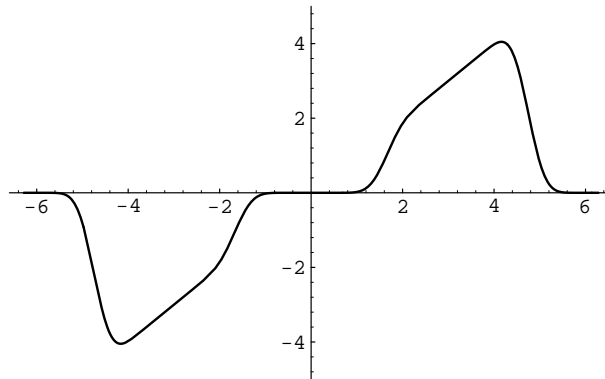


Figure 3: Approximate filter  $m_3(\xi)$  in (5.2) for the derivative of the autocorrelation of the Daubechies wavelet with 6 vanishing moments



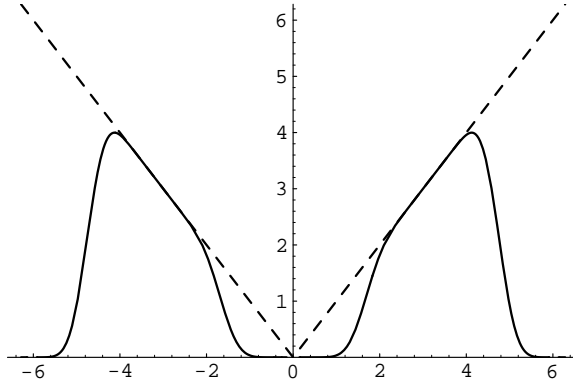


Figure 5: Approximate filter  $im_5(\xi)$  in (5.10) and the symbol  $|\xi|$  for autocorrelation of the Daubechies wavelet with 5 vanishing moments.

the evaluation of the Fourier coefficients yields

$$\left\{ \begin{array}{l} \mu_0 = \frac{\pi}{2} \\ \mu_{4k} = 0 \\ \mu_{2(2k-1)} = -\frac{\pi}{2} a_{2k-1} \\ \mu_{2k-1} = -\frac{1}{\pi} \left[ \left( \frac{2}{2k-1} \right)^2 - \sum a_{2\ell-1} \frac{(2\ell-1)^2 + \left( \frac{2k-1}{2} \right)^2}{\left( (2\ell-1)^2 - \left( \frac{2k-1}{2} \right)^2 \right)^2} \right] \end{array} \right. \quad (5.10)$$

The graph of  $im_5(\xi)$  is shown in Figure 5, together with that of  $|\xi|$ .

#### V.4 Fractional derivatives

Contrary to what the name suggests, it is better to view fractional derivatives as integral operators since they are non-local in a way similar to the Hilbert transform. This non-local behavior is manifested in the Fourier domain by the action of the operator that “breaks” the function at  $\xi = 0$ . However, in the wavelet representations such operators are approximately local if applied to functions which do not have projections on the coarsest subspace. In particular, band-limited signals are an example of such class of functions. The projection on the coarsest subspace has to be treated separately (if necessary) and requires very few operations since the function is represented by a small number of samples.

Using the following definition of fractional derivatives,

$$(\partial_x^\alpha f)(x) = \int_{-\infty}^{+\infty} \frac{(x-y)_+^{-\alpha-1}}{\Gamma(-\alpha)} f(y) dy, \quad (5.11)$$

where  $\alpha \neq 1, 2, \dots$  (if  $\alpha < 0$ , then (5.11) defines fractional anti-derivatives), we find its representation in the Fourier domain as

$$a(\xi) = e^{-i\alpha\pi/2} \xi_+^\alpha + e^{i\alpha\pi/2} \xi_-^\alpha, \quad (5.12)$$

where  $\xi_+^\alpha = \xi^\alpha$  for  $\xi > 0$  and is zero otherwise, and  $\xi_-^\alpha = |\xi|^\alpha$  for  $\xi < 0$  and is zero otherwise. Since

$$\partial_x^\alpha \Psi_{jk} = 2^{-\alpha j} (\partial_x^\alpha \Psi)_{jk}, \quad (5.13)$$

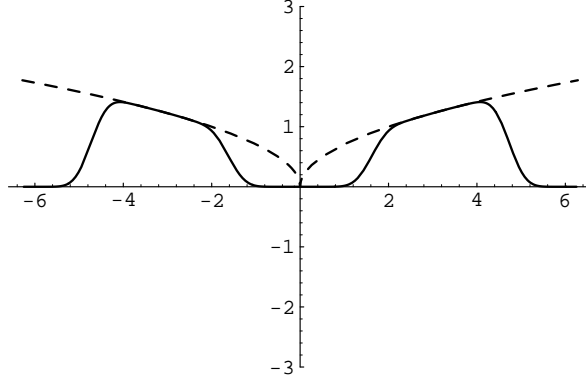


Figure 6: Modulus of the approximate filter  $m_6(\xi)$  in (5.14) for the derivative of order  $1/2$  of the Hilbert transform of autocorrelation of Daubechies' wavelet with 6 vanishing moments (dashed line: the symbol  $\xi^{1/2}$ ).

it is sufficient to evaluate the operator on the function  $\Psi$ . We have, as before,

$$m_6(\xi) = \sum_{k=-\infty}^{\infty} a(\xi + 4\pi k) |m_1(\xi + 4\pi k)|^2 \chi_{[-2\pi, 2\pi]}(\xi + 4\pi k). \quad (5.14)$$

The Fourier coefficients of  $m_6(\xi)$  are given by

$$\gamma_\ell = \frac{1}{4\pi} \int_{-2\pi}^{2\pi} a(\xi) |m_1(\xi)|^2 e^{-i\ell\xi/2} d\xi = \frac{1}{2\pi} \mathcal{R}e \int_0^{2\pi} |m_1(\xi)|^2 e^{-i\alpha\pi/2} \xi^\alpha e^{-i\ell\xi/2} d\xi. \quad (5.15)$$

Setting

$$u_k^\alpha = \frac{1}{4\pi} \int_0^{2\pi} \xi^\alpha \cos\left(\frac{k\xi + \alpha\pi}{2}\right) d\xi, \quad (5.16)$$

we obtain

$$\gamma_\ell = u_\ell^\alpha - \frac{1}{2} \sum_k a_{2k-1} \left( u_{\ell+2(2k-1)}^\alpha + u_{\ell-2(2k-1)}^\alpha \right). \quad (5.17)$$

Again, the decay of the  $\gamma_\ell$  coefficients is governed by the regularity of  $m_6$ . Since the  $2\pi$ -periodic function  $|m_1(\xi)|^2$  vanishes at  $\xi = 0$  and  $\xi = 2\pi$  together with its derivatives of order up to  $L - 1$ , one directly obtains the asymptotics of  $\gamma_\ell$ ,

$$\gamma_\ell = O(\ell^{-L-1}) \quad (5.18)$$

As an example, we display in Figure 6 the derivative of order  $\alpha = 1/2$  using the autocorrelation of Daubechies' wavelets with 6 vanishing moments. We note that  $m_6(\xi)$  is complex-valued.

## V.5 Integration operators

Let us now consider integration operator with symbol

$$\sigma(\xi) = \frac{1}{i\xi}. \quad (5.19)$$

The same procedure as before yields

$$m_7(\xi) = \frac{1}{i\xi} |m_1(\xi)|^2 = \sum_k \lambda_k \sin\left(\frac{k\xi}{2}\right). \quad (5.20)$$

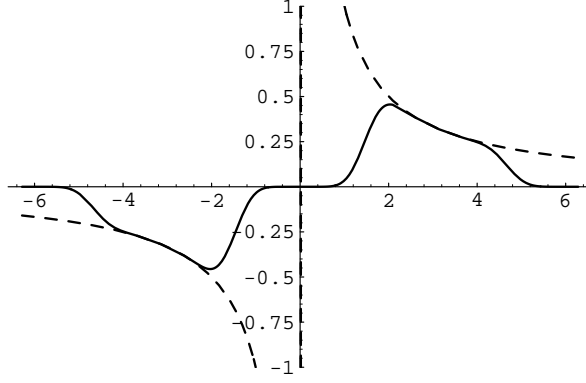


Figure 7: Approximate filter  $im_7(\xi)$  in (5.20) and the symbol  $1/\xi$  for the primitive of the autocorrelation of the Daubechies wavelet with 5 vanishing moments.

For the coefficients  $\lambda_k$ , we obtain

$$\lambda_k = \frac{-i}{2\pi} \left( Si(k\pi) - \frac{1}{2} \sum_{\ell} a_{2\ell-1} [Si((k + 2(2\ell - 1))\pi) - Si((k - 2(2\ell - 1))\pi)] \right), \quad (5.21)$$

where

$$Si(x) = \int_0^x \frac{\sin(y)}{y} dy .$$

The graph of  $im_7(\xi)$  is shown in Figure 7, together with that of  $1/\xi$ .

## VI THE HILBERT TRANSFORM OF SIGNALS

We now turn to signal processing problems. The purpose of this Section is to illustrate one of the applications of our method for computing the Hilbert transform of a signal. As we shall see, it is interesting to work in a context in which the scaling function has vanishing moments, since the samples of the signal may then be identified (within a certain accuracy) with the coefficients of its projection onto some  $\mathbf{V}_j$  space<sup>2</sup>. For this reason we shall use autocorrelation wavelets (other choices such as high order Battle-Lemarié wavelets or Coiflets, whose scaling function also possess vanishing moments, would do the job as well). The autocorrelation wavelets also offer an advantage of a trivial reconstruction formula (simple summation of wavelet coefficients over scales, see equation (9.31) in Appendix, the price to pay being an  $O(N \log(N))$  complexity).

### VI.1 Band-pass signals

Let  $f \in C^r(\mathbb{R})$ ,  $r > L$ , and assume also that  $\mathcal{H}f \in C^{r'}(\mathbb{R})$ , with  $r' > L$ . Then, according to (9.31), we have the following wavelet decompositions (we refer to (9.28) and (9.29) in Appendix for the description of our notation),

$$f(k) = S_{j_0}f(k) + O(2^{j_0(L-1)}) \quad (6.1)$$

$$= S_Jf(k) + \sum_{j=j_0+1}^J T_jf(k) + O(2^{j_0(L-1)}) \quad (6.2)$$

$$[\mathcal{H}f](k) = S_{j_0}[\mathcal{H}f](k) + O(2^{j_0(L-1)}) \quad (6.3)$$

$$= S_J[\mathcal{H}f](k) + \sum_{j=j_0+1}^J T_j[\mathcal{H}f](k) + O(2^{j_0(L-1)}) \quad (6.4)$$

But the Hilbert transform is anti self-adjoint,

$$T_j[\mathcal{H}f](k) = \langle \mathcal{H}f, \psi_{jk} \rangle = -\langle f, [\mathcal{H}\psi]_{jk} \rangle, \quad (6.5)$$

so that for  $-j_0$  large enough we have

$$[\mathcal{H}f](k) \approx S_J[\mathcal{H}f](k) + \sum_{j=j_0+1}^J W_jf(k), \quad (6.6)$$

where  $W_jf$  is defined in (4.4). We then obtain the following

**Theorem VI.1** *Let  $f \in C^r(\mathbb{R})$  be such that  $\mathcal{H}f \in C^{r'}(\mathbb{R})$ , with  $r, r' > L$ . Then*

$$[\mathcal{H}f](n) = S_J[\mathcal{H}f](n) + \sum W_jf(n) + O((1 + 2\pi)^{-\alpha L}). \quad (6.7)$$

Therefore, as long as for a sufficiently sparse scale  $J$  the low-pass component  $S_Jf(k)$  of a signal  $f(k)$  can be neglected, the algorithm in (6.7) provides a good approximation of the Hilbert transform of  $f$ .

**Remark:** The above is an  $O(N \log N)$  algorithm, because we used a redundant (without subsampling) version of wavelet decomposition algorithm. The same algorithm with subsampling requires  $O(N)$  operations, as shown in the first part of the paper.

---

<sup>2</sup>An alternative would be to use spline wavelets and the associated Lagrange interpolation to obtain the connection between approximation coefficients and samples, or to use the more general algorithms developed in [7].

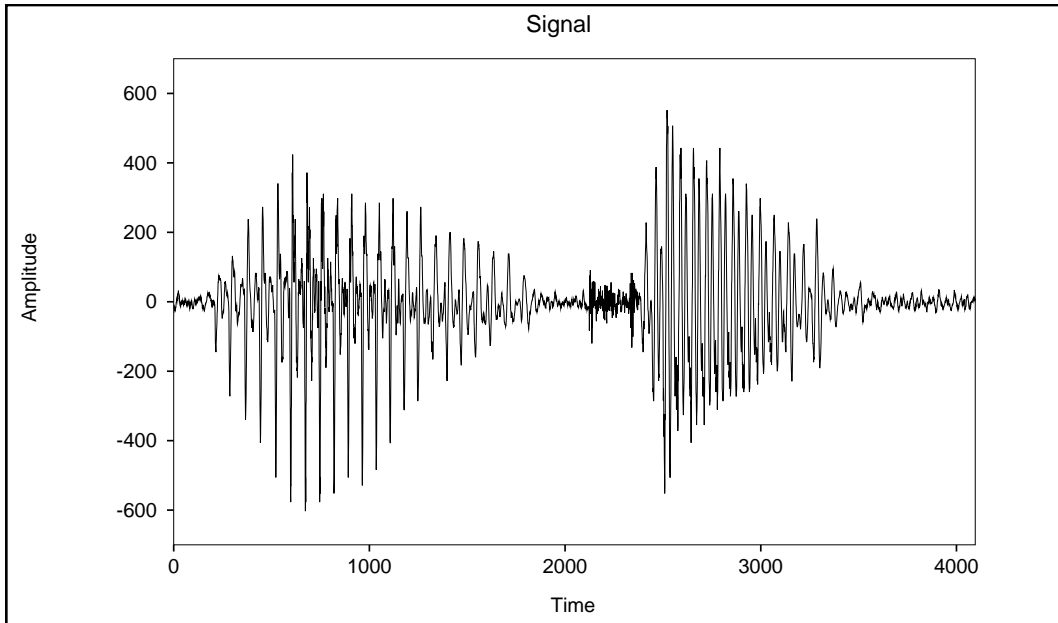


Figure 8: An example of sound /one two/ sampled at  $8kHz$ .

## VI.2 Examples

Speech signal (or at least voiced speech) is an example of signals that may be modeled as superpositions of amplitude and frequency modulated components (see e.g. [14, 12]). Although wavelet decompositions do not seem optimal for applying the analysis we have in mind to speech, let us consider it as an illustration.

In Figure 8 we show a half a second example of sound /one two/ sampled at  $8kHz$ . In Figures 9 and 10 we show the “band-pass” component of the signal  $\sum_j T_j f(n)$  and the corresponding approximate Hilbert transform  $\sum_j W_j f(n)$ , respectively. Figure 11 is a zoom of Figures 9 and 10 in which the real and imaginary parts of the reconstructed analytic signal,

$$Z_f(n) = \sum_j (T_j f(n) + iW_j f(n)) , \quad (6.8)$$

are represented. Finally, in Figure 12 we show the squared modulus  $|Z_f(n)|^2$ , i.e. the square of the instantaneous amplitude of the signal (in the sense of Ville [22]). Notice that the instantaneous amplitude still has a lot of oscillations characteristic of the presence of many additive components in the signal within the considered frequency band.

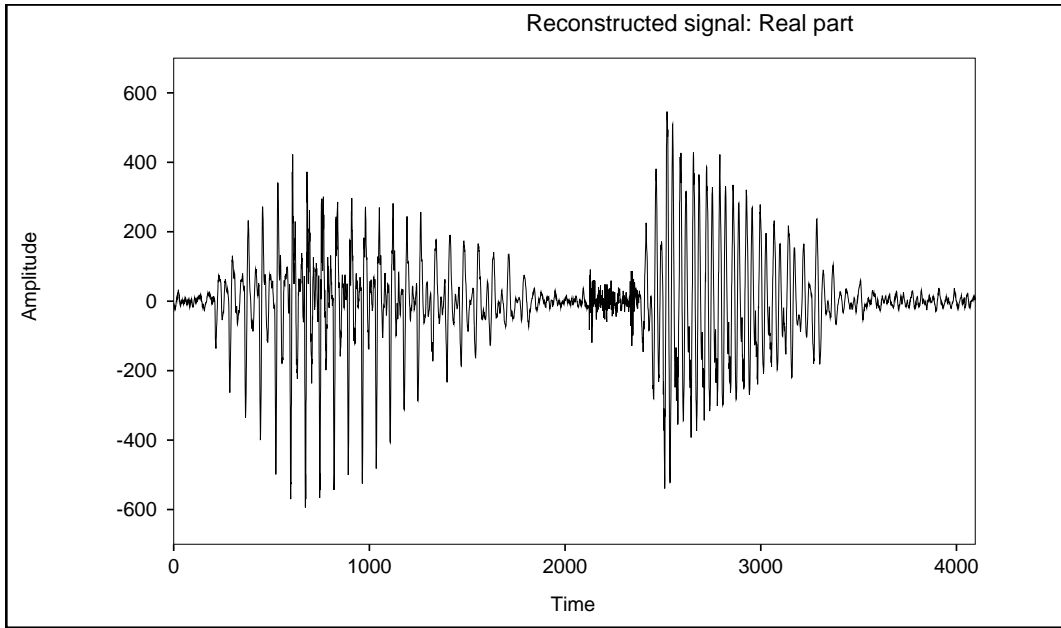


Figure 9: Real part of the reconstructed signal in (6.8).

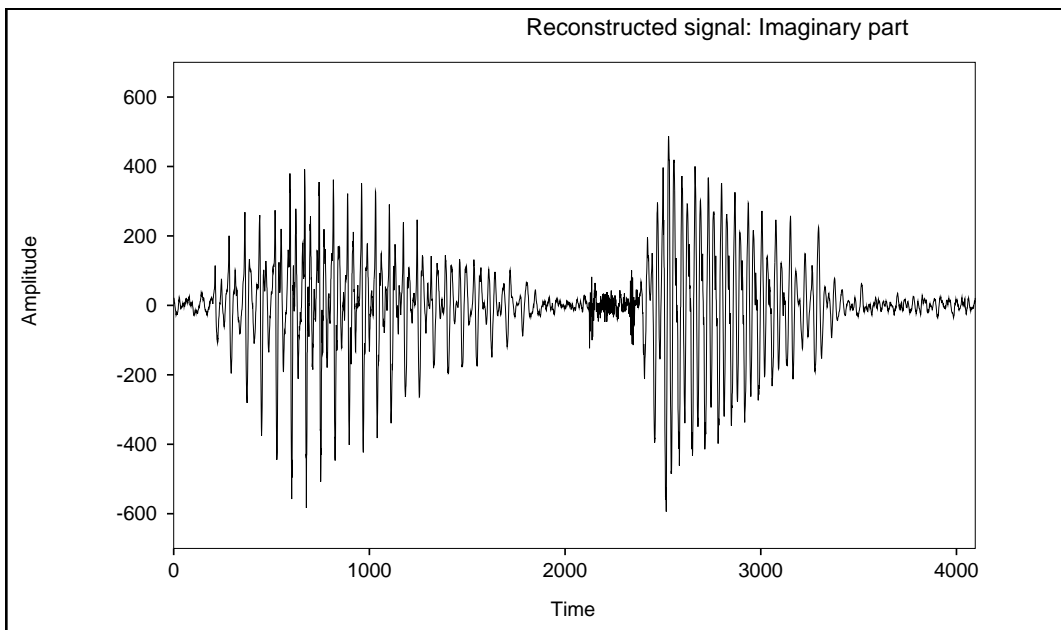


Figure 10: Imaginary part of the reconstructed signal in (6.8).

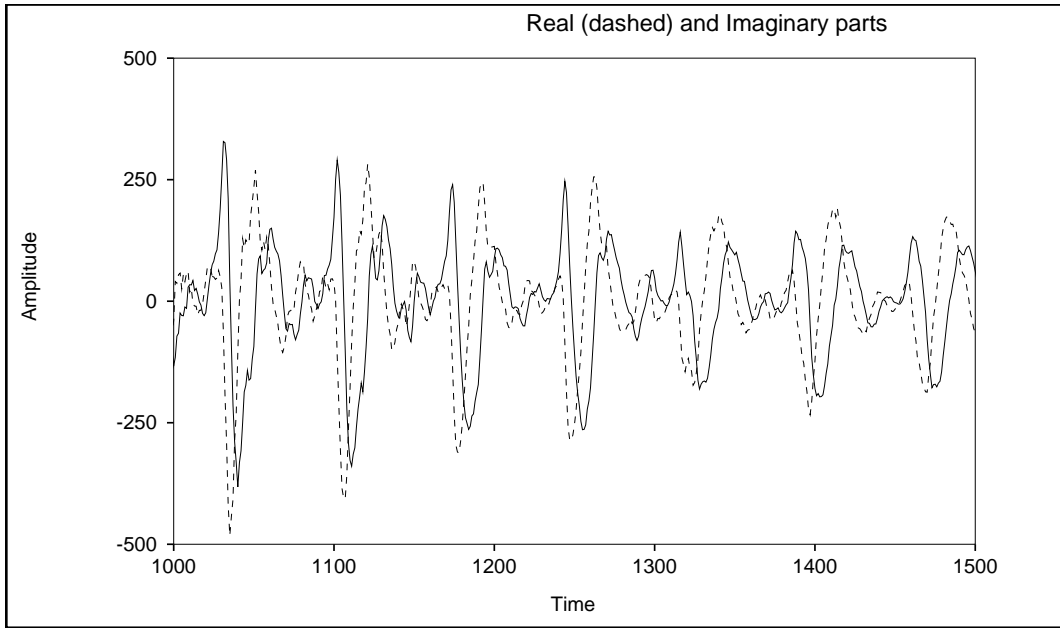


Figure 11: Zoom of real and imaginary parts of the reconstructed signal in (6.8).

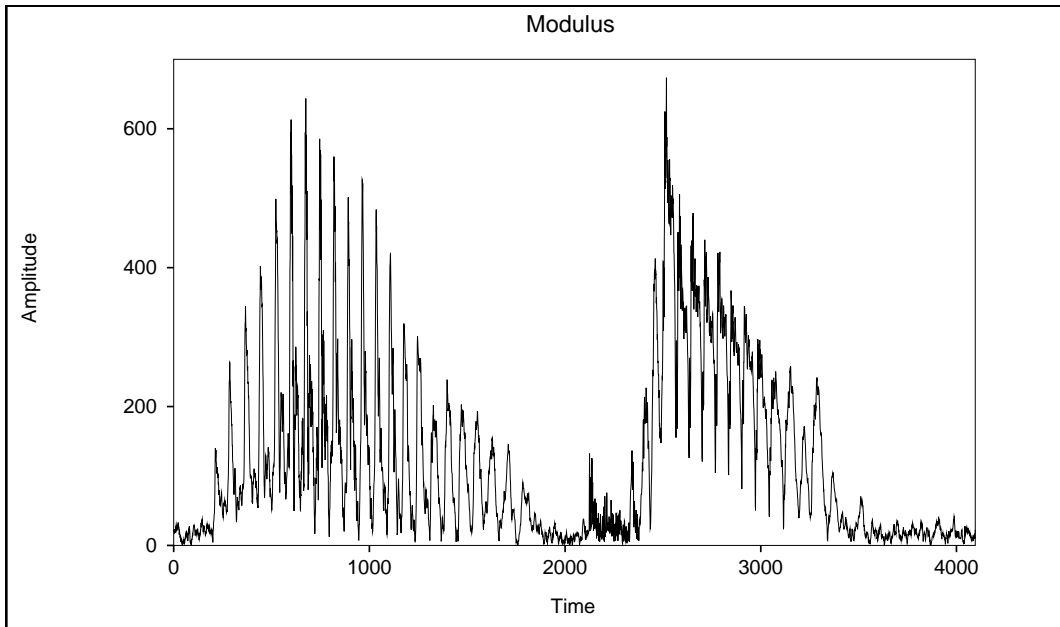


Figure 12: Modulus of the reconstructed signal in (6.8).

## VII ON THE REPRESENTATION OF SIGNALS BY LOCAL PHASES AND AMPLITUDES

It is well-known that an arbitrary continuous-time signal may be represented (e.g. using the method described in the previous Section) in terms of its local phase or its phase derivative, the instantaneous frequency, and local amplitude (following the pioneering work of J. Ville [22]).

More precisely, writing

$$Z_f(x) = f(x) + i[\mathcal{H}f](x) , \quad (7.9)$$

we obtain an analytic function (the so-called analytic signal) which may be associated with the so-called *canonical pair*,

$$\begin{aligned} A_f(x) &= |Z_f(x)| && \text{instantaneous amplitude ,} \\ \omega_f(x) &= \arg Z_f(x) && \text{instantaneous phase.} \end{aligned} \quad (7.10)$$

The instantaneous frequency is then defined as

$$\nu_f(x) = \frac{1}{2\pi} \omega'_f(x) . \quad (7.11)$$

The purpose of such representation is to obtain the local phase and amplitude in the hope that they are much less oscillatory than the original signal (and then more easily compressible if the target application is compression). Moreover, in such a case, the instantaneous amplitude and frequency are often intimately connected with physical quantities.

In general, however, the instantaneous frequency and amplitude may be as complicated as the signal itself. This is particularly clear in the example shown in the previous section (see Figure 12), where the global amplitude of the considered speech signal has fast oscillations.

An explanation of this fact is as follows. In the speech signal, a given phoneme may often be modelled as a superposition of short chirps, each having its own instantaneous frequency. It is then clear that there is no natural way of assigning a unique instantaneous frequency to such a phoneme, since the instantaneous frequency oscillates fast due to the interferences between chirps. An adequate description of the speech signal thus has to take into account this “multicomponent” character of the signal.

It is natural to expect that by splitting the frequency band, the amplitudes of the subbands will have slower oscillations, so that the representation of the subbands in terms of local phase and amplitude becomes useful. Moreover, if the considered subband “contains” one and only one of the chirps of the phoneme, standard approximations (see for instance [6, ?]) show that analytic signal provides a good approximation of the behavior of the component.

It turns out that in the discrete case such representation is quite easy to obtain from our approximate Hilbert transform algorithm. Indeed, the main aspect of our approach is to derive approximate expressions for the Hilbert transform of the wavelet  $\Psi(x)$ , together with a fast algorithm for the computation of the corresponding coefficients.

As a by-product, our method yields a decomposition of band-pass signals as

$$f(n) = \mathcal{R}e \sum_j Z_j f(n) , \quad (7.12)$$

where

$$Z_j f(n) = T_j f(n) + iW_j f(n) \quad (7.13)$$

may be thought of as a “discrete analytic subband” of the signal. Again, it is easy to obtain from such analytic subbands the local amplitudes and frequencies,

$$\begin{aligned} A_j f(n) &= |Z_j f(n)|, \\ \nu_j f(n) &= \frac{1}{2\pi} \left( \frac{T_j f(n) W_j f'(n) - T_j f'(n) W_j f(n)}{A_j f(n)^2} \right). \end{aligned} \quad (7.14)$$

Expression in (??) and (7.14) is a discrete approximation of the continuous expression for the instantaneous frequency of an analytic signal. In particular, it involves the derivatives of  $T_j f$  and  $W_j f$  which may be evaluated using the representation of the derivative in bases of compactly supported wavelets derived in [2].

As an example in Figure 13, we illustrate the representation of the scale decomposition of the speech signal /one two/ sampled at 8kHz. Plots represent coefficients  $T_j f(n)$  and the corresponding local amplitudes  $A_j f(n)$ , respectively. In computations, we used autocorrelations of Daubechies’ wavelet with 9 vanishing moments. It turns out that each one of the  $T_j f$  signals has a much simpler structure than the original signal itself, so that its local amplitude is a much more natural object than the global one. It is reasonable to expect that this method could be used as a method for compression (a non-linear compression scheme). Indeed, the local amplitudes and frequencies being slowly varying, are easier to compress. We also see a potential for feature extraction (for example speaker identification in speech processing, along the lines of [12]).

Let us stress that the results of this paper may be generalized to wavelet packet decompositions (see e.g. [23]), where the wavelet basis appears as a particular case of a family (library) of orthonormal basis decompositions generated from a pair of quadrature mirror filters. For this purpose we have a triplet of filters  $m_0(\xi)$ ,  $m_1(\xi)$ ,  $m_2(\xi)$  from which we may generate all wavelet packets and their (approximate) Hilbert transform. This permits us to look for the decomposition that is optimal in terms of information cost (within the above-mentioned non-linear compression scheme) for a given signal. We plan to address this problem elsewhere.

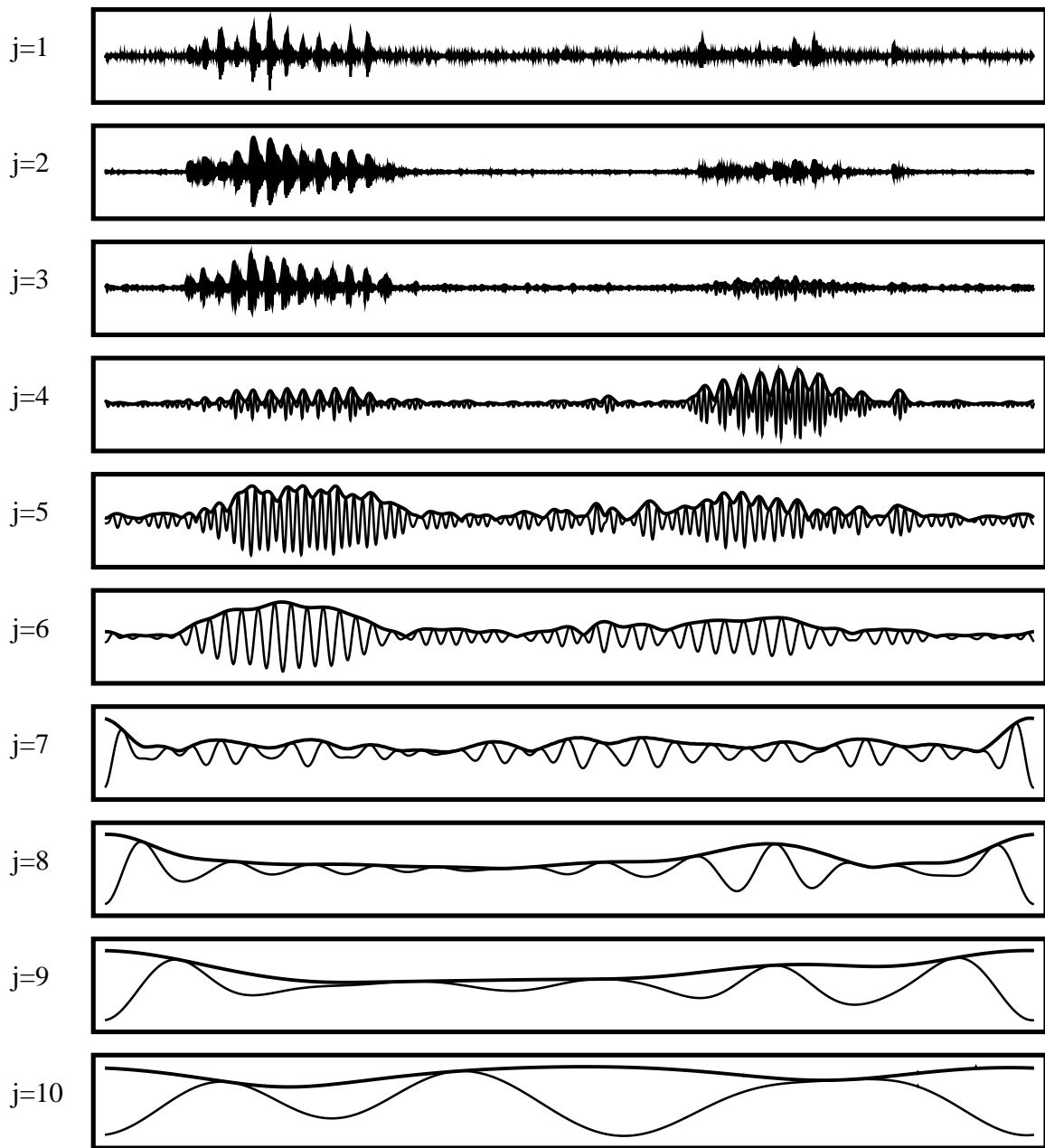


Figure 13: Scale decomposition of the /one two/ signal

## VIII CONCLUSIONS

We have described here a method for approximating the action of a class of operators on wavelets, and obtained several fast effective algorithms for the numerical evaluation of such operators in the form of filter banks. Such algorithms are easy to implement in both software and hardware. The operators under consideration are essentially convolution operators, i.e. operators characterized by a multiplier in the Fourier domain, and we described a possible extension to some classes of pseudodifferential operators. Our method has to be thought of as an alternative to the NS-form approach in [3]. Indeed, we demonstrate that we obtain the same results with comparable accuracy.

Our construction is illustrated using the “autocorrelation wavelets” described in [19], but may be applied to any wavelet decomposition associated with quadrature mirror filters with several vanishing moments. It is worth noticing that the underlying approximation are quite close to those made in [17] for finding approximate fast wavelet transform algorithms.

In the case of the Hilbert transform, the results of Section VII clearly indicate that the representation of signals by local amplitude and phase is in general not appropriate, since it yields a fast oscillating amplitude (and frequency). However, it appears likely that this difficulty may be avoided by associating amplitude and phase to the subbands of the signal. Such method may be developed in the framework of our approach, which we plan to address separately in regards to speech processing applications.

### **Acknowledgments.**

The research of G.B. was partially supported by ARPA grant F49620-93-1-0474 and ONR grant N00014-91-J4037.

## References

- [1] P. Auscher. Il n'existe pas de base d'ondelettes régulières dans l'espace de Hardy  $H^2(\mathbb{R})$ . *C.R.Acad.Sci. Paris*, 315(1):769–772, 1992.
- [2] G. Beylkin. On the representation of operators in bases of compactly supported wavelets. *SIAM J. Numer. Anal.*, 29(6):1716–1740, 1992.
- [3] G. Beylkin, R. R. Coifman, and V. Rokhlin. Fast wavelet transforms and numerical algorithms I. *Comm. Pure and Appl. Math.*, 44:141–183, 1991. Yale University Technical Report YALEU/DCS/RR-696, August 1989.
- [4] J. Carrier, L. Greengard, and V. Rokhlin. A fast adaptive multipole algorithm for particle simulations. *SIAM Journal of Scientific and Statistical Computing*, 9(4), 1988. Yale University Technical Report, YALEU/DCS/RR-496 (1986).
- [5] I. Daubechies. *Ten Lectures on Wavelets*. CBMS-NSF Series in Applied Mathematics. SIAM, 1992.
- [6] N. Delprat, B. Escudié, P. Guillemain, R. Kronland-Martinet, Ph. Tchamitchian, and B. Torrèsani. Asymptotic wavelet and Gabor analysis: extraction of instantaneous frequencies. *IEEE Trans. Inform. Theory*, 38:644–664, 1992. Special issue on wavelet and multiresolution analysis.
- [7] B. Delyon and A. Juditsky. On the computation of wavelet coefficients. Technical Report 1994/PI-856, IRISA, Campus de Beaulieu, 35042 Rennes Cedex, France, 1994.
- [8] D.Esteban and C. Galand. Application of quadrature mirror filters to split band voice coding systems. *International Conference on Acoustics, Speech and Signal Processing*, pages 191–195, 1977. Washington, D.C.
- [9] L. Greengard and V. Rokhlin. A fast algorithm for particle simulations. *J. Comp. Phys.*, 73(1):325–348, 1987.
- [10] A. Grossmann, R. Kronland-Martinet, and J. Morlet. Reading and understanding continuous wavelet transforms. In J.M. Combes, A. Grossmann, and P. Tchamitchian, editors, *Wavelets: Time-Frequency Methods and Phase Space*, pages 2–20. Springer-Verlag, 1989.
- [11] P.G. Lemarié-Rieusset. Sur l'existence des analyses multirésolution en théorie des ondelettes. *Revista Matemática Iberoamericana*, 8(3):457–474, 1992.
- [12] S. Maes. *The Wavelet Transform in Signal Processing, with Applications to the Extraction of Speech Modulation Model Features*. Dissertation, Université Catholique de Louvain, Louvain la Neuve, Belgium, 1994.
- [13] S. Mallat. Multiresolution approximation and wavelets. Technical report, GRASP Lab, Dept. of Computer and Information Science, University of Pennsylvania.
- [14] R.J. McAulay and T.F. Quatieri. Low rate speech coding based on the sinusoidal model. In S. Furui and M. Mohan Sondui, editors, *Advances in Speech Signal Processing*, 1992.
- [15] Y. Meyer. Ondelettes et fonctions splines. Technical report, séminaire edp, Ecole Polytechnique, Paris, France, 1986.

- [16] Yves Meyer. *Ondelettes et Opérateurs*. Hermann, Paris, 1990.
- [17] M.A. Muschietti and B. Torresani. Pyramidal algorithms for littlewood-paley decompositions. *SIAM J. Math. Anal.*, *submitted*, 1993. preprint.
- [18] V. Rokhlin. Rapid solution of integral equations of classical potential theory. *J. Comp. Phys.*, 60(2), 1985.
- [19] N. Saito and G. Beylkin. Multiresolution representations using the auto-correlation functions of compactly supported wavelets. *Submitted to IEEE Transactions on Signal Processing*, 1991. Also Research Note at Schlumberger-Doll Research, Ridgefield, CT, 1991 and in Proceedings of ICASSP-92, 4:381-384.
- [20] M. J. Smith and T. P. Barnwell. Exact reconstruction techniques for tree-structured subband coders. *IEEE Transactions on ASSP*, 34:434–441, 1986.
- [21] J. O. Stromberg. A Modified Franklin System and Higher-Order Spline Systems on  $\mathbf{R}^n$  as Unconditional Bases for Hardy Spaces. In *Conference in harmonic analysis in honor of Antoni Zygmund, Wadsworth math. series*, pages 475–493, 1983.
- [22] J. Ville. Théorie et Applications de la Notion de Signal Analytique. *Cables et Transmissions*, *2nd year*, 1:61–74, 1948.
- [23] M. V. Wickerhauser. *Adapted Wavelet Analysis from Theory to Software*. A.K. Peters, Boston, 1994.

## IX Appendix: Wavelet bases and Multiresolution Analysis

### IX.1 Multiresolution Analysis

Let us introduce our notation. We will work in the context of multiresolution analysis [13] and [15],

$$\dots \subset \mathbf{V}_2 \subset \mathbf{V}_1 \subset \mathbf{V}_0 \subset \mathbf{V}_{-1} \subset \mathbf{V}_{-2} \subset \dots \subset \mathbf{L}^2(\mathbb{R}) , \quad (9.1)$$

with the scaling function  $\phi(x)$  and wavelet  $\psi(x)$ , and define subspaces  $\mathbf{W}_j$  as orthogonal complements of  $\mathbf{V}_j$  in  $\mathbf{V}_{j-1}$ ,

$$\mathbf{V}_{j-1} = \mathbf{V}_j \oplus \mathbf{W}_j . \quad (9.2)$$

We set

$$\begin{cases} \psi_k^j(x) &= 2^{-j/2} \psi(2^{-j}x - k) \\ \phi_k^j(x) &= 2^{-j/2} \phi(2^{-j}x - k) \end{cases} \quad (9.3)$$

and expand any  $f \in L^2(\mathbb{R})$  as

$$\begin{aligned} f(x) &= \sum_{j,k \in \mathbf{Z}} d_k^j \psi_k^j(x) \\ &= \sum_{k \in \mathbf{Z}} s_k^{j_0} \phi_k^{j_0}(x) + \sum_{j < j_0} \sum_{k \in \mathbf{Z}} d_k^j \psi_k^j(x) , \end{aligned} \quad (9.4)$$

where

$$\begin{cases} d_k^j &= \langle f, \psi_k^j \rangle \\ s_k^j &= \langle f, \phi_k^j \rangle . \end{cases} \quad (9.5)$$

As usual, there exist  $2\pi$ -periodic trigonometric polynomials  $m_0(\xi)$  and  $m_1(\xi)$  such that

$$\begin{aligned} \hat{\phi}(2\xi) &= m_0(\xi) \hat{\phi}(\xi) \\ \hat{\psi}(2\xi) &= m_1(\xi) \hat{\phi}(\xi) , \end{aligned} \quad (9.6)$$

where  $\hat{\phi}$  and  $\hat{\psi}$  are the Fourier transforms of  $\phi$  and  $\psi$ , *e.g.*,

$$\hat{\phi}(\xi) = \int_{\mathbb{R}} \phi(x) e^{-i\xi x} d\xi . \quad (9.7)$$

Filters  $m_0$  and  $m_1$  satisfy the “exact reconstruction condition”,

$$|m_0(\xi)|^2 + |m_1(\xi)|^2 = 1 . \quad (9.8)$$

Let us denote by  $H = \{h_\ell\}_{\ell=0}^{L-1}$  and  $G = \{g_\ell\}_{\ell=0}^{L-1}$  the associated quadrature mirror filters. A direct consequence of equation (9.6) is the pyramidal algorithm for the computation of the coefficients

$$\begin{cases} s_k^j &= \sum_{\ell} h_\ell s_{2k-\ell}^{j-1} \\ d_k^j &= \sum_{\ell} g_\ell s_{2k-\ell}^{j-1} , \end{cases} \quad (9.9)$$

which requires  $O(N)$  operations and may be viewed as a convolution followed by decimation (or downsampling). The same filters are used in the reconstruction algorithm (again an  $O(N)$  algorithm),

$$s_k^j = \sum_{\ell} \left( h_{2\ell-k} s_\ell^{j+1} + g_{2\ell-k} d_\ell^{j+1} \right) , \quad (9.10)$$

which may be viewed as upsampling followed by convolution.

In the signal processing part of the paper we use the *dyadic wavelet transform*, a “translation-invariant” version of multiresolution decompositions. In such a case, one considers all the integral translates of the wavelet and the scaling function, i.e.

$$\begin{cases} \psi_{jk}(x) &= 2^{-j/2}\psi(2^{-j}(x-k)) \\ \phi_{jk}(x) &= 2^{-j/2}\phi(2^{-j}(x-k)) \end{cases} . \quad (9.11)$$

The corresponding coefficients of  $f \in \mathbf{L}^2(\mathbb{R})$  are denoted by

$$\begin{cases} d_{jk} &= \langle f, \psi_{jk} \rangle \\ s_{jk} &= \langle f, \phi_{jk} \rangle , \end{cases} \quad (9.12)$$

and their numerical evaluation may be realized via an  $O(N \log(N))$  algorithm similar to (9.9),

$$\begin{cases} s_{jk} &= \sum_{\ell} h_{\ell} s_{j-1, k-2^{j-1}\ell} \\ d_{jk} &= \sum_{\ell} g_{\ell} s_{j-1, k-2^{j-1}\ell} . \end{cases} \quad (9.13)$$

We denote by  $M$  be the number of vanishing moments of  $\psi(x)$ , i.e.,

$$\int_{\mathbb{R}} x^m \psi(x) dx = 0, \quad m = 0, 1, \dots, M-1, \quad (9.14)$$

and consider compactly supported wavelets and associated quadrature mirror filters. The filter coefficients  $G$  inherit the vanishing moments from the wavelet, namely,

$$\sum_{\ell} \ell^m g_{\ell} = 0, \quad m = 0, 1, \dots, M-1. \quad (9.15)$$

## IX.2 Autocorrelation Shell

We also develop the algorithm for the Hilbert transform in the context of the autocorrelation shell described in [19], where the wavelet and scaling functions are autocorrelations of the wavelet and scaling function associated with I. Daubechies’ wavelets (see e.g. [5]).

Let  $m_0(\xi)$  and  $m_1(\xi)$  be the  $2\pi$ -periodic square-integrable quadrature mirror filters associated with an orthonormal basis of compactly supported wavelets. Let us denote by  $\phi$  and  $\psi$  associated scaling function and wavelet, respectively. Let  $\Phi(x)$  and  $\Psi(x)$  denote the autocorrelation functions of  $\phi(x)$  and  $\psi(x)$ . Then we have

$$\widehat{\Phi}(\xi) = \prod_{j=1}^{\infty} |m_0(2^{-j}\xi)|^2, \quad (9.16)$$

and

$$\widehat{\Psi}(\xi) = \left| m_1\left(\frac{\xi}{2}\right) \right|^2 \cdot \widehat{\Phi}\left(\frac{\xi}{2}\right). \quad (9.17)$$

One can immediatly see that

**Lemma IX.1** *Both  $\Phi(x)$  and  $\Psi(x)$  are interpolating functions, i.e.*

$$\Phi(n) = \Psi(n) = \delta_{n,0}. \quad (9.18)$$

Thus, we have for functions on the subspace spanned by  $\{\Phi(2^j x - k)\}_{k \in \mathbf{Z}}$ ,

$$f(x) = \sum_k f(2^{-j}k)\Phi(2^j x - k). \quad (9.19)$$

If  $\{h_k\}_{k=0}^{L-1}$  are the Fourier coefficients of  $m_0(\xi)$ , then one has the following two-scale difference equations:

$$\Phi(x) = \Phi(2x) + \frac{1}{2} \sum_{\ell=1}^{L/2} a_{2\ell-1} [\Phi(2x - 2\ell + 1) + \Phi(2x + 2\ell - 1)], \quad (9.20)$$

$$\Psi(x) = \Phi(2x) - \frac{1}{2} \sum_{\ell=1}^{L/2} a_{2\ell-1} [\Phi(2x - 2\ell + 1) + \Phi(2x + 2\ell - 1)], \quad (9.21)$$

where

$$a_k = 2 \sum_{\ell=0}^{L-1-k} h_\ell h_{\ell+k}. \quad (9.22)$$

In the Fourier domain, we have

$$|m_0(\xi)|^2 = \frac{1}{2} + \frac{1}{2} \sum_{k=1}^{L/2} a_{2k-1} \cos(2k-1)\xi, \quad (9.23)$$

and

$$|m_1(\xi)|^2 = \frac{1}{2} - \frac{1}{2} \sum_{k=1}^{L/2} a_{2k-1} \cos(2k-1)\xi. \quad (9.24)$$

Clearly,  $\hat{\Psi}(\xi) \sim \xi^L$  as  $\xi \rightarrow 0$ , so that  $\Psi(x)$  has  $L$  vanishing moments. In addition, it is easy to see that the scaling function also has vanishing moments,

$$\int x^m \Phi(x) dx = 0, \quad m = 1, \dots, L-1. \quad (9.25)$$

We will need in the sequel the following properties of the sequence  $\{a_{2\ell-1}\}$ :

**Lemma IX.2** 1.  $\sum_1^{L/2} a_{2\ell-1} = 1$ .

2.  $\sum_1^{L/2} (2\ell-1)^{2m} a_{2\ell-1} = 0, \quad m = 1, \dots, L/2-1$ .

*Proof:*

Since the function  $\Psi(x)$  has  $L$  vanishing moments, we have

$$0 = \int \Psi(x) dx = \int \Phi(2x) dx - \frac{1}{2} \sum_1^{L/2} a_{2\ell-1} \int [\Phi(2x - 2\ell + 1) + \Phi(2x + 2\ell - 1)] dx, \quad (9.26)$$

which implies the first property. On the other hand, using (9.25) for  $2, 4, \dots, 2m-2$ ,  $m < L/2$ ,

one has

$$\begin{aligned}
0 &= \int x^{2m} \Psi(x) dx \\
&= \int x^{2m} \Phi(2x) dx - \frac{1}{2} \sum_1^{L/2} a_{2\ell-1} \int x^{2m} [\Phi(2x - 2\ell + 1) + \Phi(2x + 2\ell - 1)] dx \\
&= \int x^{2m} \Phi(2x) dx - \frac{1}{2} \sum_1^{L/2} a_{2\ell-1} \int \left[ \left(x + \ell - \frac{1}{2}\right)^{2m} \Phi(2x) + \left(x - \ell + \frac{1}{2}\right)^{2m} \Phi(2x) \right] dx \\
&= - \sum_1^{L/2} \left(\ell - \frac{1}{2}\right)^{2m} a_{2\ell-1} \int \Phi(2x) dx ,
\end{aligned} \tag{9.27}$$

which implies the second property.

If  $f \in L^2(\mathbb{R})$ , we will denote by  $T_j f$  and  $S_j f$  the dyadic wavelet transform of  $f$  and the scaling function transform of  $f$ ,

$$S_j f(x) = 2^{-j} \int f(y) \Phi(2^{-j}(y-x)) dy , \tag{9.28}$$

$$T_j f(x) = 2^{-j} \int f(y) \Psi(2^{-j}(y-x)) dy . \tag{9.29}$$

We have

**Lemma IX.3** *Let  $f \in C^r(\mathbb{R})$ , with  $r \geq L$ . Then  $S_j f(n) = f(n) + O(2^{j(L-1)})$ .*

The two-scale difference equations imply that the computation of the  $S_j f(n)$  and  $T_j f(n)$  coefficients can be realized through the following pyramidal algorithm,

$$\begin{cases} S_j f(n) &= S_{j-1} f(n) + \frac{1}{2} \sum_{\ell} a_{2\ell-1} (S_{j-1} f(n - 2\ell + 1) + S_{j-1} f(n + 2\ell - 1)) \\ T_j f(n) &= S_{j-1} f(n) - \frac{1}{2} \sum_{\ell} a_{2\ell-1} (S_{j-1} f(n - 2\ell + 1) + S_{j-1} f(n + 2\ell - 1)) . \end{cases} \tag{9.30}$$

Moreover, the perfect reconstruction formula (9.8) yields the following simple reconstruction formula from the autocorrelation wavelet coefficients,

$$S_0 f(n) = \sum_{j=0}^{\infty} T_j f(n) . \tag{9.31}$$